A Catalog of New Eclipsing Binaries in the *Kepler* Database

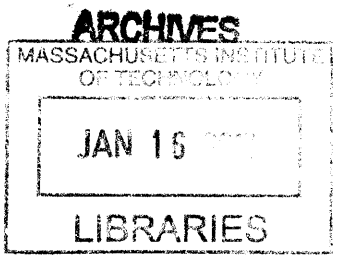

by

Michael Christopher Kotson

Submitted to the Department of Physics
in partial fulfillment of the requirements for the degree of

Bachelor of Science in Physics

at the

MASSACHUSETTS INSTITUTE OF TECHNOLOGY

June 2012

Author .....
Department of Physics
May 17, 2012

Certified by.....
Saul A. Rappaport
Professor Emeritus
Thesis Supervisor

A Catalog of New Eclipsing Binaries in the *Kepler* Database

by

Michael Christopher Kotson

Submitted to the Department of Physics
on May 17, 2012, in partial fulfillment of the
requirements for the degree of
Bachelor of Science in Physics

Abstract

In this thesis, we present a catalog of binary stars discovered in the publicly available *Kepler* database, none of which were included in previous such catalogs published by the *Kepler* science team. A brief review of other binary star catalogs is given, including the Prša et al. catalog on which we are expanding. We detail the means by which the *Kepler* data were downloaded and reduced to produce light curves, and we explain the FFT selection algorithm and visual inspections which were used to find new candidates for binary systems. Finally, the classifications by which these candidates were sorted are explained in full, and the binary catalog itself is presented as Appendix A. In all, we found 173 new binary systems not listed in the *Kepler* team's binary catalog of 2,176 systems. We were also able to successfully find ~1,400 of the 2,074 binary stars which the *Kepler* team had identified and which were available in the public *Kepler* data release, thereby providing some indication of the efficiency of our search. Further appendices list RR Lyrae type stars found during the research and peculiar objects of interest which may merit further study.

Thesis Supervisor: Saul A. Rappaport
Title: Professor Emeritus

Acknowledgments

The author would like to extend his thanks to Dr. Robert Szabo of the Konkoly Observatory in Budapest, Hungary, for his help in identifying a few of the more unusual light curves we encountered during this study. We are also grateful to Dr. Katrien Kolenberg of Harvard and Dr. Gerald Handler of the Copernicus Astronomical Center in Poland for providing similar help. Dr. Handler also helped us in our study of KIC 7740983, and in particular, with the evolution of the folded light curves as a function of time. The object is discussed in Appendix C. And of course, the author extends his deepest gratitude to Dr. Alan Levine and Prof. Saul Rappaport for welcoming him on to their team and directing this research. Prof. Rappaport's assistance in compiling and revising this thesis is especially appreciated.

Contents

List of Figures

List of Tables

Chapter 1

Introduction

1.1 Binary Stars and Catalogs

Of the various methods used to determine the physical parameters of stars, such as their masses and radii, the study of light curves produced by observations of eclipsing binary systems is exceptionally straightforward and direct. And because knowledge of these physical parameters is crucial to determining distances and the theoretical development of stellar evolution, any catalog which lists examples of these eclipsing binary systems would prove to be a worthwhile astrophysical tool.

A binary system consists of two stars - the more massive star is usually called the "primary" and its partner the "secondary" - orbiting about their common center of mass. In the special case where the line of sight to the system lies roughly in the system's orbital plane, each star will periodically block some or all of the light from its companion star from reaching the observer; such stars comprise what is known as an eclipsing binary (EB) system. By combining photometric and spectroscopic observations (to produce light curves and radial-velocity curves, respectively), it is possible to accurately determine the masses, radii, and luminosities of each component star of an eclipsing binary, which facilitates studies of stellar structure and evolution [Andersen, 1991]. The same physical parameters, in principle, can be used to determine the distance to an eclipsing binary by comparing the luminosity of each star to its apparent brightness. Applications of this method have allowed distances to

neighboring galaxies to be determined to an impressive 5% accuracy [Bonanos, 2006].

Several catalogs of binary systems have been compiled to aid astronomical studies. The first were created in the late 18^{th} Century by William Herschel, who observed and published catalogs of approximately 700 double stars (stars which are seen near to each other in the sky). A number of these stars were later determined to be bound physical binary systems via astrometric studies [Heintz, 1978]. More modern efforts include the Washington Double Star Catalog[1], an ongoing project of the US Naval Observatory which has measured the separations, magnitudes, spectral types, and proper motions of 115,769 systems; the Budding et al. "Catalogue of Algol-type binary stars"[2], which provides information on 411 semi-detached binary stars and was last updated in 2004; and the 1980 Brancewicz and Dworak "Catalogue of Parameters for Eclipsing Binaries"[3], which contains the physical and geometric parameters of 1048 eclipsing binaries. Furthermore, the General Catalog of Variable Stars (GCVS)[4], which is a reference source of all presently known variable stars, also contains many binaries in its catalog of ~46,000 systems[5].

Also, many catalogs of extragalactic EBs have been constructed to aid distance measurements. Most notable are the catalogs constructed as byproducts of gravitational microlensing surveys of the Large and Small Magellanic Clouds (LMC and SMC). While searching for evidence of massive compact halo objects, projects such as the Microlensing Observations in Astrophysics experiments and OGLE-II Project have discovered a total of approximately 1300 EBs in the SMC and 2500 in the LMC; the MACHO project has revealed an additional 2000 binaries in the LMC [Bonanos, 2006].

Projects intended to search for exoplanets have also found some success in cataloging binary stars. These include the ground-based SuperWASP mission, which has so far identified at least 53 binaries [Norton et al., 2011], and the satellite-based CoRoT mission, which has published its own light curve studies of binaries discovered

[1] http://www.usno.navy.mil/USNO/astrometry/optical-IR-prod/wds/WDS
[2] http://vizier.cfa.harvard.edu/viz-bin/ftp-index?J/A+A/417/263
[3] http://vizier.cfa.harvard.edu/viz-bin/ftp-index?II/150A
[4] http://heasarc.gsfc.nasa.gov/W3Browse/all/gcvs.html
[5] http://www.sai.msu.su/gcvs/gcvs/intro.htm

in its field of view [Maciel et al.].

Note that all of these catalogs arose from studies which were not originally intended to discover EBs. Any collection of precise time-series photometric data on a field of stars can be used to search for new binaries and construct such a catalog. This includes the light curves released by the *Kepler* mission, which was launched with the purpose of discovering Earth-like exoplanets but nonetheless provides all the resources necessary to identify and classify binary systems.

While the lists above may seem to imply that binary systems are well-monitored and further catalogs are unnecessary, none of these projects had photometric precision nearly as high as those available from the *Kepler* mission. The unprecedented photometric precision of the *Kepler* detectors (measured in 10-100 parts per million) above the Earth's scintillating atmosphere have provided an incredible opportunity to further study the light curves of binary star systems with previously unattainable accuracy. For this reason, a collection of binary star classifications and measurements derived from the available *Kepler* light curves should provide an invaluable addition to the study of binary systems.

This work is meant to expand upon one such catalog, initially published by Andrej Prša and the *Kepler* team in February 2011 [Prša et al., 2011] and developed further in November of the same year [Slawson et al., 2011]. Specifically, by combining a selection algorithm based on Fourier transformations of *Kepler* light curves with a follow-up visual inspection of the phase-folded light curves, this catalog has been created to identify EB systems which were missed by the Prša et al. study.

In chapter two of this thesis, we detail the methods by which the *Kepler* data were prepared for inspection in Fourier space, as well as the qualifications used to identify periodically variable systems.

Chapter three describes and provides illustrative examples of the different searches which were performed to find new EB candidates, including searches for non-EB systems which were nonetheless interesting and could possibly merit further investigation.

The complete catalog itself is available in Appendix A. The catalog lists the iden-

tifying Kepler Input Catalog ("KIC") numbers, periods, radii, temperatures, and tentative classifications of all confirmed binary systems. Appendix B provides a similar catalog for RR Lyrae type stars we have identified in the *Kepler* data, and Appendix C contains figures illustrating some other interesting objects which were encountered during this study.

1.2 The *Kepler* Mission

NASA's *Kepler* satellite was launched on 6 March, 2009, with the stated goal of identifying planets (especially those with Earth-like properties) in orbit around other stars in the Milky Way[6]. The method by which *Kepler* detects an exoplanet is entirely photometric: when a planet passes in front of its host star and the observer, it blocks a portion of the star's light, and this "transit" event is evident as a dip in the star's brightness[7]. This is closely related to the means by which EB systems are detected, so the light curves released by the *Kepler* mission can serve the additional purpose of EB discovery.

The search for planets by the *Kepler* team has so far produced 2,321 planet candidates around 1,790 separate stars according to Batalha et al., 2012[8]. Figure 1-1 shows how these planet candidates are distributed by orbital period.

1.2.1 The Satellite

The *Kepler* satellite (see Figure 1-2, from the *Kepler* Quick Guide[9]) occupies an Earth-trailing heliocentric orbit so as to allow near-continuous observation of the same field in Cygnus-Lyra (see Figure 1-3, from the MAST Archive[10]). This field covers a large 100 square degrees of the sky containing well over 100,000 stars above 16^{th} magnitude, the light from which is captured by a 1.4 meter primary mirror and a total of 95 mega pixels spread among 42 CCDs.

[6] http://www.nasa.gov/mission_pages/kepler/launch/index.html
[7] http://kepler.nasa.gov/Mission/QuickGuide/
[8] http://archive.stsci.edu/kepler/planet_candidates.html
[9] http://kepler.nasa.gov/Mission/QuickGuide/
[10] http://archive.stsci.edu/kepler/images/New_FOV_6m.pdf

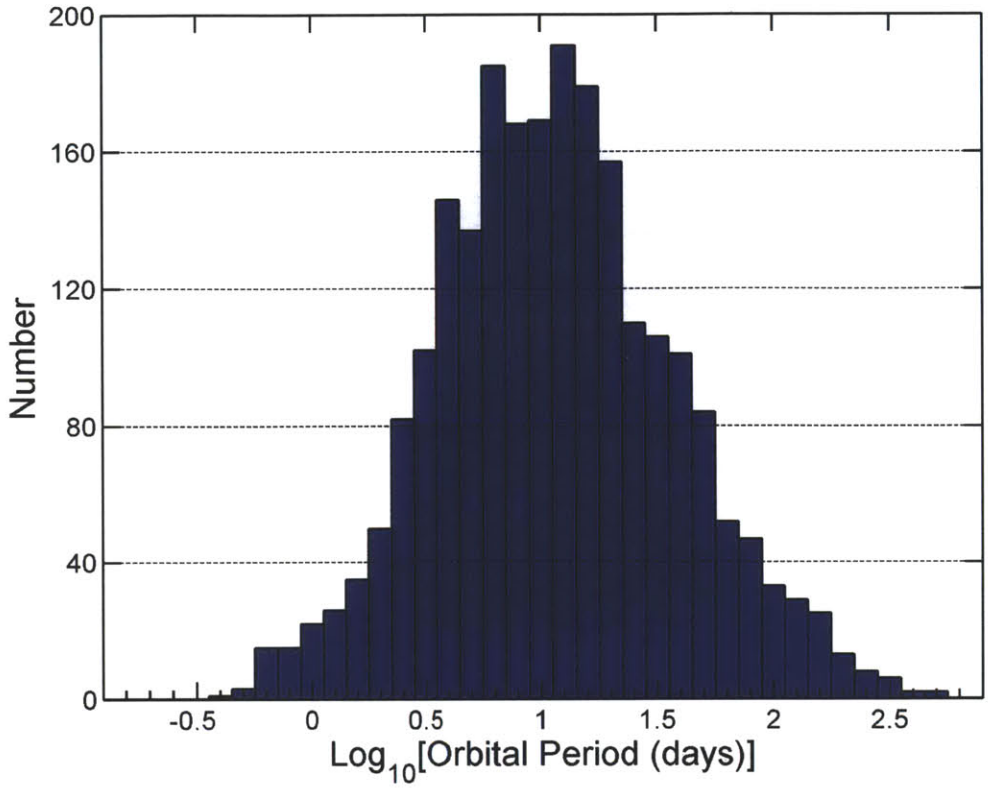

Figure 1-1: The distribution of *Kepler* planetary candidates by orbital period, using the catalog provided by Batalha et al., 2012.

Kepler's original intended lifetime was 3.5 years, though the mission has recently been extended beyond that. Its operation is only interrupted for data downlinks (monthly) and 90 degree rotations every three months to keep its solar arrays pointed toward the sun. It is able to observe stars between 8^{th} and 16^{th} magnitude to the precision necessary to detect transits of Earth-sized planets, which often produce decreases in flux of less than 0.1% or even 0.01%.

1.2.2 Prša's Catalog

The *Kepler* team led by Andrej Prša has published a catalog of 2165 EB systems discovered in the Quarter 2 (Q2) *Kepler* data [Slawson et al., 2011], expanding upon their previous catalog of 1879 systems [Prša et al., 2011]. Among other parameters,

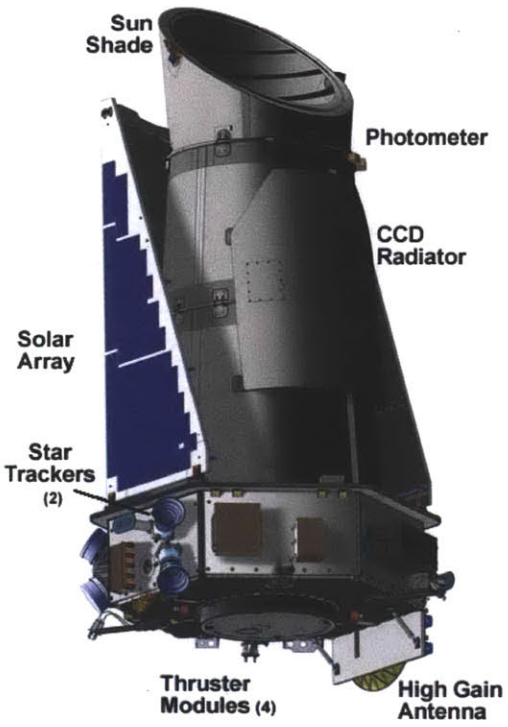

Figure 1-2: An artist's conception of the *Kepler* Spacecraft, including illustrations of its photometer. (Image courtesy of NASA's *Kepler* Quick Guide.)

this catalog lists the period, effective temperature, B-V color, and some orbital parameters of each identified system. Furthermore, most systems are classified by the separation of the constituent stars relative to their radii, from over-contact (OC), to semi-detached (SD), to detached (D). Prša also identifies binary systems in which there are no eclipses, but which are thought to be binary because of the so-called "ellipsoidal light variations" (ELV) caused by their gravitational interaction.

Our preliminary searches through the same Q2 data revealed a number of clear EB systems which were not included in the catalog. These objects have been classified, to the best of the author's ability, according to the same scheme used by Prša et al. The catalog constructed in this thesis, therefore, is an attempt to modestly expand upon and clarify the work conducted by Prša, so the two catalogs can be considered together as a somewhat more complete and accurate list of EB systems in the *Kepler* field of view.

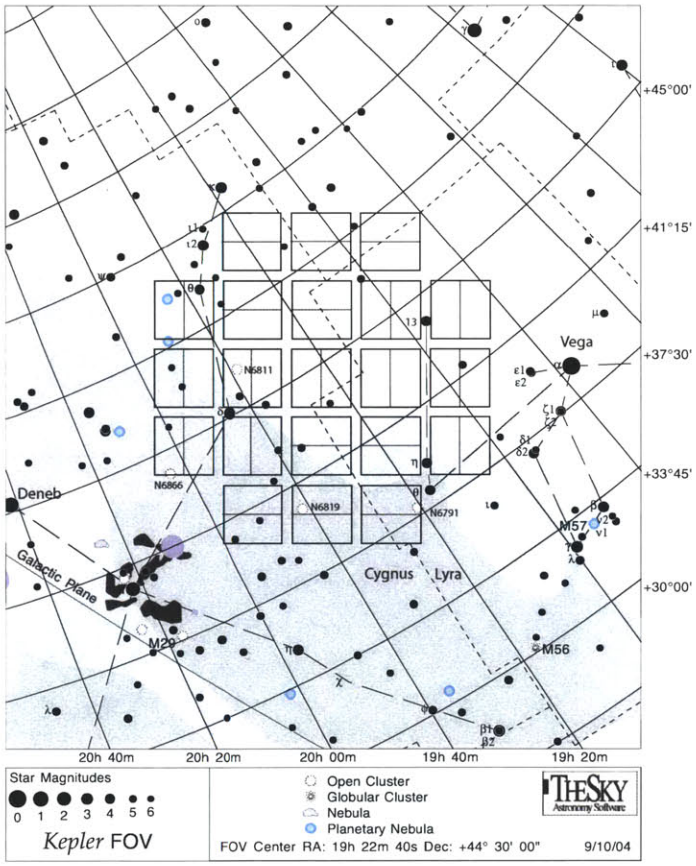

Figure 1-3: The field of view of the *Kepler* satellite, courtesy of the MAST Archive. The 42 rectangles show how *Kepler*'s 42 CCDs are arranged in the focal plane.

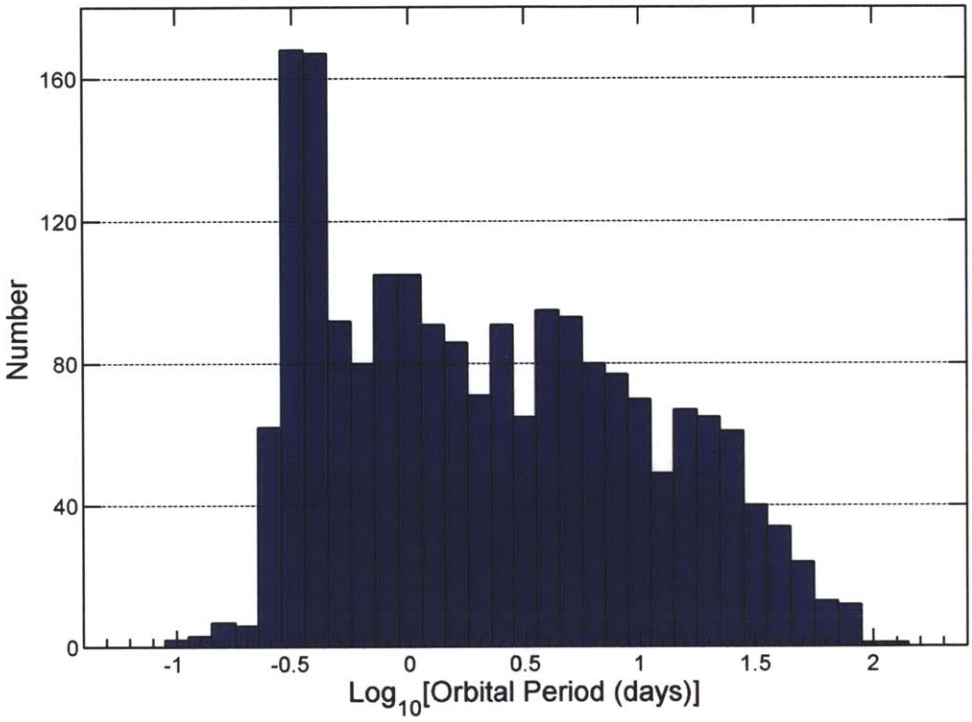

Figure 1-4: The distribution of orbital periods among the objects listed in the most recent *Kepler* binary star catalog.

Chapter 2

Data Reduction and Processing

This chapter will detail the means by which the light curve data were obtained from the *Kepler* database and the methods of reduction used to correct unphysical trends in these data and convert them into a more usable form. In addition, the procedure that was followed to detect the harmonics expected in the light curves of binary or planetary systems will be thoroughly described. This technique succeeded in analyzing ~160,000 *Kepler* targets and producing summary plots of 4,674 candidates as potential eclipsing binaries. As we shall see, this number still includes a large number of false positives (for reasons to be explained). Chapter 3 will describe the search performed on this shortened list of light curves to identify objects of interest.

All computations were performed using the IDL programming language.

2.1 Data Download and Description

All light curve data were downloaded in FITS format from the Quarter 2 publicly released data available at the Multimission Archive at STScI (MAST)[1] as of September 2010. At the time of its initial release, this set contained data from ~160,000 stars and star systems observed between 20 June and 16 September 2009 (an 88-day interval). As reserved targets have become public, the number of available FITS files has increased slightly.

[1] `http://keplergo.arc.nasa.gov/ArchivePublicDataQ2.shtml`

Table 2.1: Utilized Data Fields of *Kepler* FITS

Data Field	Description
BARYTIME	Barycentric corrected, reduced Julian day
AP_RAW_FLUX	Aperture photometry "uncorrected" flux
AP_CORR_FLUX	Aperture photometry processed for planetary search
TEFF	Derived effective temperature
LOGG	Derived log10 surface gravity
RADIUS	Estimated stellar radius

A single FITS file provides the measured values of a wide range of physical parameters of the star system, as well as the measurements of time and flux necessary to construct a light curve. A summary of the available data fields which were of importance to this research is provided in Table 2.1. Some gaps and anomalies in the data are present, but are well-understood as systematic effects due to the repositioning and maintenance of the *Kepler* satellite, as detailed in the *Kepler* Data Release 7 notes [Christiansen and Machalek, 2010]. Light curve data are reported in either short- (SC) or long-cadence (LC) period, with SC data coadded in 58.85-second intervals and LC data coadded in 1766-second (or 0.49-hour) intervals. As such, any separation betweeen two consecutive data points in a single light curve which is greater than the standard cadence qualifies as a gap, and no two consecutive data points are separated by less than the light curve's standard cadence.

From the fields of data available in the downloaded FITS files, only BARYTIME and AP_CORR_FLUX were used in the frequency-space search for eclipsing candidates, though AP_RAW_FLUX was often studied in case physical trends in the flux data were accidentally removed by the *Kepler* team's correction algorithms. For the remainder of this thesis, references to the "flux" of a system will be to the data from AP_CORR_FLUX unless otherwise noted.

2.2 Data Reduction and Transformation

Even for the corrected flux data, some procedures had to be followed to remove artifacts and prepare the data for a discrete Fourier transform. The most common

artifacts encountered were flux data points whose values were missing and hence set equal to (-INF). These points stand as markers for the gaps in the data due to the systematic processes in the *Kepler* data pipeline explained above and can be safely ignored [Christiansen and Machalek, 2010]. Any such data points - and their corresponding points from BARYTIME - were removed from the flux before further processing.

Next, the discrepancies in the cadence of each individual light curve - the amount of time separating any two consecutive data points - had to be reconciled. By construction, the fast Fourier transform (FFT) assumes equal spacing between data points on the time axis. Otherwise, the linear correlation between bin number and time is broken, and the resultant frequencies reported out of the FFT will be invalid.

Each light curve was reconstructed by dividing the time series into a number of bins whose widths were equal to the standard cadence of the light curve in question (utilizing a slight modification of code the author had constructed for a previous project). If the portion of the time series to which a bin corresponded contained a data point, the flux value of this data point was assigned to the bin. If the bin corresponded to a gap in the time series, it was assigned the flux value of the last bin before the gap. That is, if bin n had a flux value of f, but the next x consecutive bins $n+1, n+2, ...n+x$ each corresponded to no flux value, all x empty bins were assigned a flux of f. This correction was expected to minimize the window-function artifacts introduced into the FFT.

The final alterations made to the light curve were meant to remove any linear trends, as linear rises or falls in flux over an 88-day period could be attributed to instrumental drifts for all cases of interest to this research. A linear approximation was fit to each curve and subsequently divided out of the flux. The flux was then normalized, with its maximum value set to unity, so the relative changes in brightness could be more easily evaluated.

With the gaps in its cadence corrected and all linear trends removed, each light curve was ready to be studied in frequency space. To achieve this, a simple FFT was performed on the reduced flux data after subtracting out the mean flux to center the

data about zero. The modulus of the FFT was then calculated to combine the sine and cosine components inferred from the complex FFT. In all frequency-space plots presented in this thesis, the y-axis (often referred to as "amplitude") corresponds to this modulus, not to the modulus-squared (or "power") as is common practice.

2.3 Analysis and Candidate Determination

In the following subsections we describe (i) the coarse-grained screening algorithm which detected harmonics in frequency space, (ii) the quick visual inspection to discard false positives; and (iii) the phase-folding of all surviving candidates about the period(s) detected in the FFTs. These inspections of the reduced data and FFTs (obtained by the methods described in the previous section) determined whether or not each light curve represented an EB or other interesting periodically variable system.

2.3.1 The FFT Selection Algorithm

As illustrated in Figure 2-1, the dips that are representative of EB systems can be recognized in frequency-space by the distinctive pattern of equally-spaced FFT "peaks" they produce. The first of these peaks occurs at the "base frequency", which is the inverse of the orbital period, and the subsequent peaks occur at integral multiples (or "harmonics") of the base frequency. It turns out that any sharp-featured periodic dips or peaks in a light curve can be expected to produce this effect, including some stellar pulsators. However, identifying a harmonic pattern of peaks is an efficient first step in identifying a binary.

In the algorithm developed to search for harmonic patterns, a significant peak was defined to be an FFT value whose amplitude exceeded the mean amplitude of its nearest neighbors by more than a factor of 4. The definition of "nearest neighbors" varied: for the sixth to one-hundredth frequency bins, the five previous lower-frequency bins and five next higher-frequency bins were used to compute the mean; for bin number 101 to the Nyquist limiting bin, the fifteen previous lower and fifteen next higher bins were used. The averages are computed over a smaller frequency range at lower

frequencies because there are fewer bins separating the harmonics of a low-frequency signal. The first five frequency bins were ignored due to the fact that most FFTs of real data are subject to a modest amount of $1/f$ noise. The requirement of a peak that is a factor of 4 above background-noise was an arbitrary choice decided by trial-and-error. If no significant peaks were found in frequency space for a given object, the search skipped forward to the next *Kepler* target.

With the previous step completed, all significant peaks were identified and the search for harmonics could begin. Starting with the lowest-frequency peak, corresponding to a frequency bin f_0, the fifteen bins that fell in the range $\frac{1}{2}f_0 \pm 2$, $2f_0 \pm 2$, and $3f_0 \pm 2$ were identified. If the amplitude in any of these bins exceeded the mean of its nearest neighbors (defined in the same way as above) by a factor of 3, this was interpreted as a harmonic pair with the peak at f_0, and the star system in question was labeled as an EB candidate. If no such harmonic was found, the search would continue again from the next peak at f_1, then f_2 and so on. Only a single harmonic pair identification was required for EB candidacy.

2.3.2 Automation and Output

The data reduction and Fourier transformation described in Section 2.2 and the harmonic inspection described in Section 2.3.1 were performed automatically on each of the ~160,000 *Kepler* targets in succession using an IDL script. In addition, by comparing the KIC number of each target against an ASCII list of the binaries identified by the Prša team [Slawson et al., 2011] and a similar list of planetary candidates compiled by the team led by William Borucki[2], the systems which had already been included in either of these catalogs were identified by the script.

If a *Kepler* target was determined to be an EB candidate by the harmonic screening algorithm, a four-panel plot was produced to allow further inspection. The four components of the plot (an example of which can be seen in Figure 2-1) were as follows:

[2] `http://kepler.nasa.gov/files/mws/FebDataRelease_revised_020211.pdf`

1. Top Left: Uncorrected, normalized AP_RAW_FLUX versus time, with a label if the system is part of Prša's or Borucki's catalog

2. Bottom Left: AP_CORR_FLUX with cadence and linear corrections, normalized, versus time

3. Top Right: The FFT used in the selection algorithm, with the frequency axis labelled in "Cycles per Day" and extending out to the Nyquist frequency; the frequency of the "tallest" peak is noted at the top of the subplot

4. Bottom Right: Same as Top Right, but with the frequency axis only covering low-frequency behavior, allowing for closer inspection of this regime

Using the information provided by the header of the target's FITS file, the four-panel plot was also labeled with the system's TEFF, RADIUS, and LOGG values as measured by *Kepler* (see Table 2.1). It was also noted on the plot if the source appears in either the Prša or Borucki catalogs. Section 2.3.3 will explain how these plots were used for the next stage of binary identification.

2.3.3 Visual Inspection

Of the initial ~160,000 light curves, 4,674 were chosen for further consideration by the FFT selection algorithm described above. However, these included a large number of systems which were already listed in the Prša et al. catalog, as well as a substantial number of stellar pulsators. The goal of the next step of the procedure was to determine and eliminate the false positives.

A false positive is here defined as a system whose FFT shows peaks which allow it to pass the selection algorithm, but which can be determined by visual inspection not to be an EB or any of the "interesting cases" to be discussed in the next chapter. Such stars exhibit some other type of periodic behavior, such as pulsations in brightness or sunspots on their rapidly rotating surfaces.

We show an example of one of the four-panel plots in Figure 2-1 to illustrate the visual inspection process. The subject of this figure is KIC 4281068, a binary

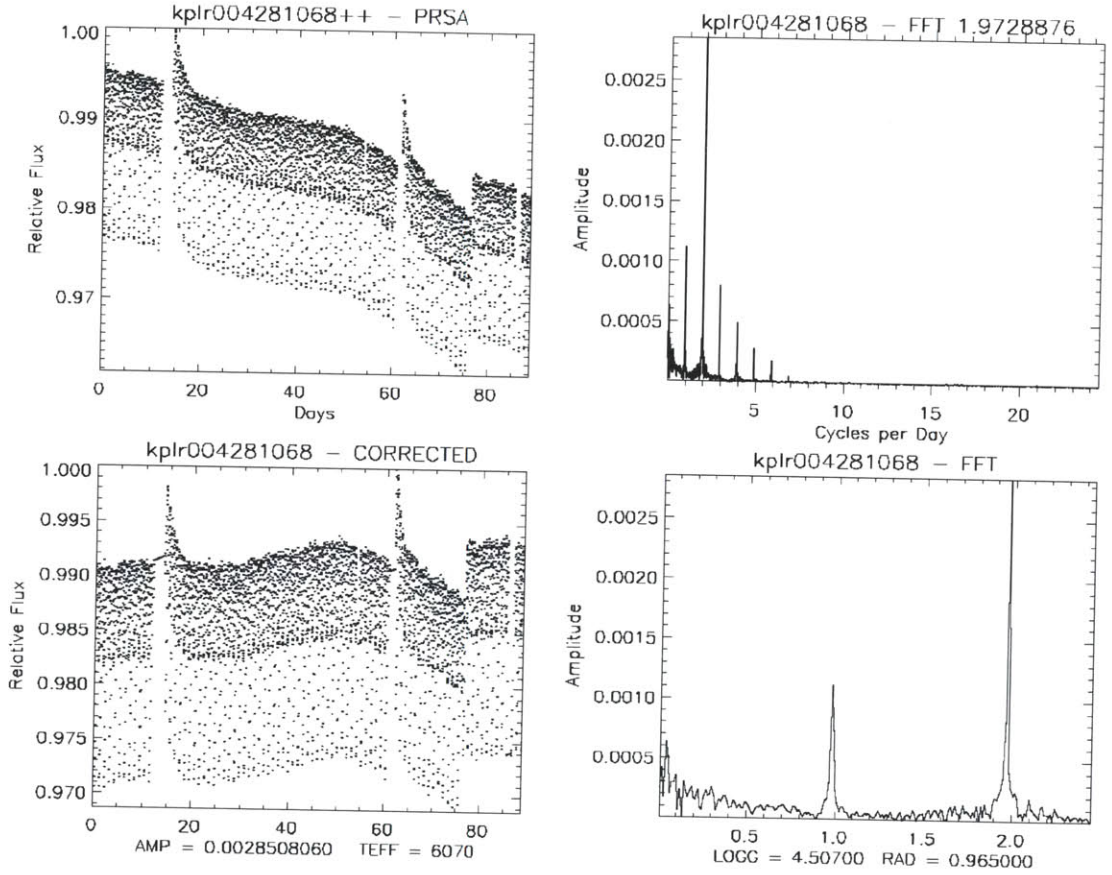

Figure 2-1: An illustrative 4-panel plot of the light curve and FFT for KIC 4281068. The panels are (counter-clockwise from the upper left): (i) the raw *Kepler* data (flux vs. time), (ii) the corrected flux, (iii) the low frequency portion of the FFT, and (iv) the entire FFT (up to the Nyquist limit of ~25 cycles/day). The pattern of peaks in the FFT is clearly representative of an EB. The two "glitches: in the data at days 15 and 82 were due to "safeholds" of the satellite and are therefore instrumental in origin.

system which is included in Prša's catalog. This is a typical FFT of an EB (of the "over-contact" variety), and the primary and secondary eclipses are fairly obvious in the light curves. The FFT peak with the greatest amplitude occurs near 1.973 cycles per day and lies at the first harmonic of the base frequency, so the period should be approximately $2 \times (1.973)^{-1}$ or 1.014 ± 0.001 days. The error on this calculation comes from the fact that each frequency bin (for a long-cadence light curve) has a width of $(1766 \text{ sec})^{-1}$ or $\sim$0.006 cycles per second, and without Fourier interpolation we obtain the frequency to better than half a bin.

As demonstrated by the phase-folded light curve in Figure 2-2, the period is approximately 1.015 days, which is in agreement with our FFT determination above. In a phase-fold, the time axis of a light curve is divided into a number of segments, each with a length equal to the period in question. These segments are then overlaid atop each other so that data points corresponding to the same phase of the orbit will overlap. Since the phase-fold of KIC 4281068 at a period of 1.015 forms a very coherent light curve with clear primary and secondary eclipses, we can confirm the system to be an EB.

On the other hand, take the case of KIC 4283747, as illustrated in Figure 2-3. There are so many random peaks in this FFT that this object passed the FFT selection algorithm by pure chance. There is no distinct harmonic pattern, so this is clearly not an EB and no coherent phase-fold can be constructed. Nor is there a pattern present that is representative of any of the special cases to be discussed in the next chapter. This system is one of many which was not of particular interest to this research, but should prove useful in asteroseismology studies.

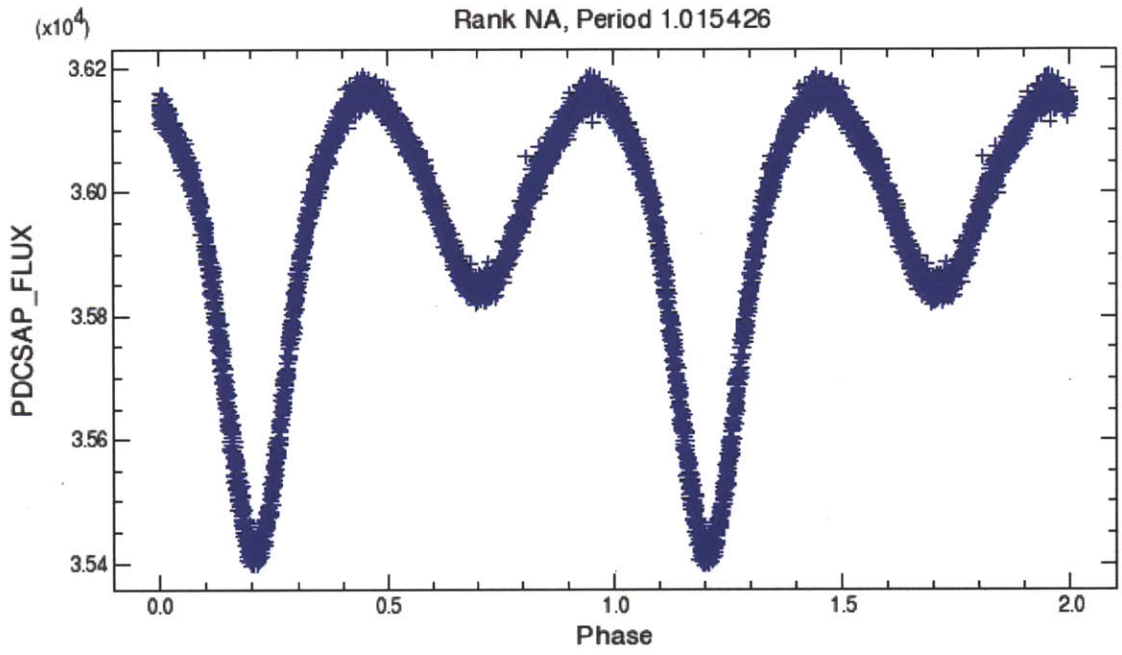

Figure 2-2: The light curve of KIC 4281068 phase-folded about the orbital period 1.015 days. The primary and secondary eclipses are clearly visible, showing that this system is an EB. It is likely that these two stars are orbiting each other essentially in Roche lobe contact.

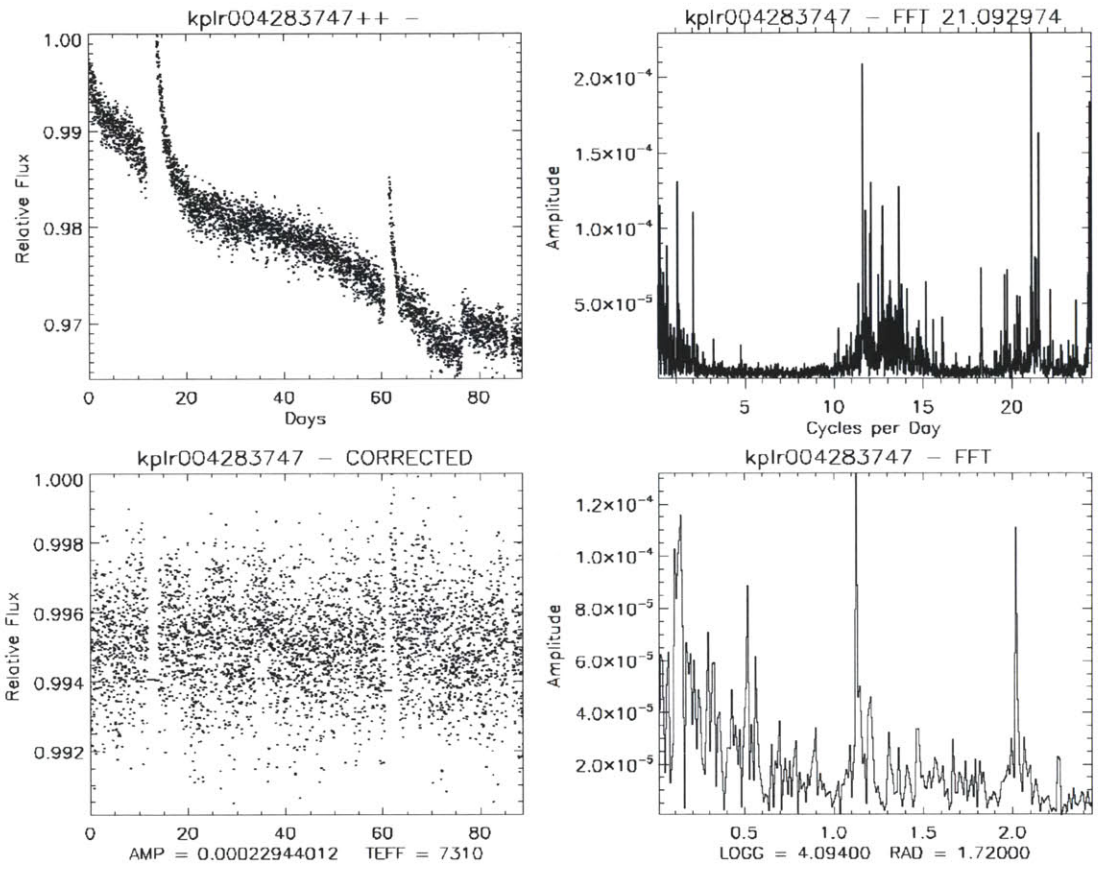

Figure 2-3: The light curve and FFT of KIC 4283747, which passed the FFT selection algorithm, but only as a false positive. The FFT is chaotic, which allowed it to exhibit one or more accidental "harmonic pairs" among its many significant peaks. Note the temperature of the star is ~7,300 K, making this a likely δ-Scuti pulsator.

2.3.4 Phase-Folding Analysis

The final step in identifying the EB systems and other interesting objects involved phase-folding the light curves which had passed the previous two screening processes. This utilized the resources available through the NASA Exoplanet Archive[3], which allows users to fold the light curve of any available *Kepler* object about a period which is calculated by a Lomb-Scargle algorithm. Further details of this method will be discussed in the next chapter.

[3] `http://exoplanetarchive.ipac.caltech.edu/applications/ETSS/Kepler\_index.html`

Chapter 3

Searching for EBs and Other Interesting Systems

The first two steps of the selection process reduced the number of EB candidates or periodically variable systems of interest from ~160,000 to ~500 (setting aside the ~1,400 objects we found that were already in the Prša catalog[1], which were tentatively assumed to be true EBs). Since this number was much more manageable than the full *Kepler* set of targets, a third step could be utilized to classify each of the remaining candidates according to the shape of its phase-folded light curve.

As mentioned in the previous chapter, all phase-folds were produced using the NASA Exoplanet Archive's Periodogram resource[2], which utilized a Lomb-Scargle algorithm to determine the most accurate period about which to fold each light curve. The Lomb-Scargle algorithm is analogous to an FFT, but is designed to work on non-uniformly spaced data [Scargle, 1982].

The sections of this chapter will describe the qualities of phase-folded light curves and FFT patterns by which certain classifications were defined. The classifications covered by this work are the following: Binary stars, RR-Lyrae pulsating stars, and

[1]While the Prša et al. catalog contains 2,176 objects at the time of this writing, only 2,074 of those were targets which were included in the publicly released Q2 data at the time of our download. Therefore, the FFT selection algorithm succeeded in identifying ~1,400 of a total possible 2,074 Prša binaries.

[2]`http://exoplanetarchive.ipac.caltech.edu/applications/ETSS/Kepler\_index.html`

sub-giant stars with solar-like oscillations. Figure 3-1 is provided as an example of the FFT patterns which are representative of each binary sub-classification.

3.1 Binary Stars

As mentioned before, a binary star system consists of a primary and a secondary star in orbit about a common center of mass. Following the lead of Prša et al., our search for these systems focused on identifying four separate classes of binaries: Detached (D), Semi-Detached (SD), Overcontact (OC), and Ellipsoidal Light Variables (ELV). The next subsection will detail the parameters by which these classes can be distinguished; the following subsections will describe how each class can be identified by studying the FFTs and phase-folds of their light curves at the orbital period.

3.1.1 Parameters of Binary Stars

It is worthwhile to note here how some physical properties of the component stars in an EB can be inferred from the light curve. This will not only explain how the study of EBs can benefit studies of stellar evolution or distance scales (which require measurements of each star's mass and radius), but it will also explain some key differences between the EB classifications soon to be discussed.

The simplest measurements to make from an EB light curve are those of the orbital period and eclipse duration. The full width of an eclipse, dT, can be determined directly from the light curve, and this can be converted to the eclipse half-angle, ϕ, as follows:

$$2\phi = 2\pi\frac{dT}{P}, \tag{3.1}$$

where P is the orbital period. In the case that the orbital inclination of the binary system is nearly 90° with a circular orbit, we can further relate the stellar radii and orbital separation to the eclipse angle by

$$\sin(\phi) = \frac{R_1 + R_2}{a}, \tag{3.2}$$

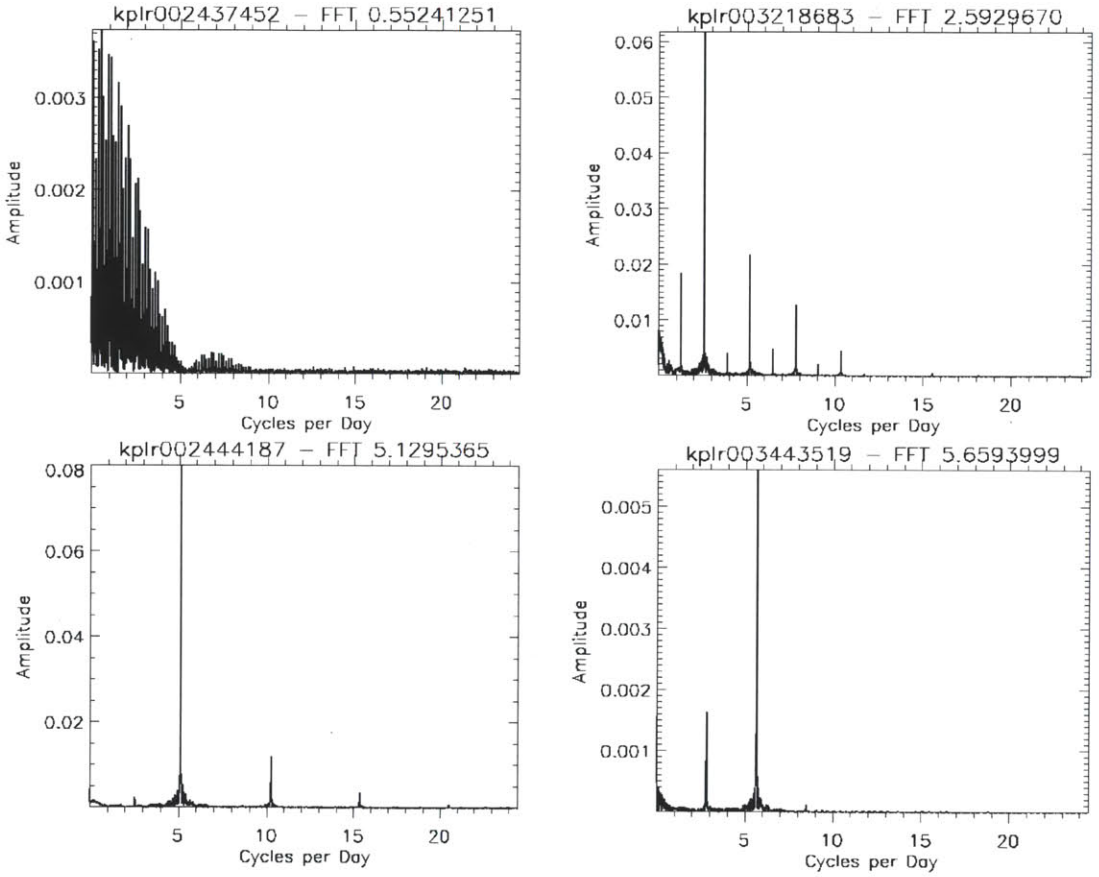

Figure 3-1: These sample FFT patterns illustrate the following (clockwise from upper left): (i) the dense envelope of peaks representative of a detached (D) binary with a long period; (ii) the harmonic pattern with a clear peak at the base frequency seen in most semi-detached (SD) binaries (here, the peak at the first harmonic is larger than that at the base frequency); (iii) the harmonic pattern with a barely discernable base frequency peak of an overcontact (OC) binary; and (iv) the FFT of an ellipsoidal light variable (ELV), with a single dominant peak at twice the base frequency and few harmonics.

with R_1 and R_2 being the radius of each constituent star and a being the separation between them. Thus the simple measurement of dT can tell how separated the stars are with respect to the sum of their radii, which is a key ratio differentiating among D, SD, and OC binaries. For eccentric and/or inclined orbits, the corresponding expressions are more complicated.

The degree to which each component star fills its Roche lobe is another key difference between the EB classifications. The Roche lobe is the critical potential surface around each star in a frame of reference that rotates with the binary. Any mass beyond this surface is subject to being lost from the system or transferred to the other star. The radius of a star's Roche lobe in units of orbital separation, R_L, depends only upon the binary system's mass ratio, q, where

$$q = M_1/M_2, \tag{3.3}$$

with M_1 being the mass of the star in question (primary or secondary) and M_2 the mass of its companion. If q is known, R_L can be approximated using Peter Eggleton's formula [Eggleton, 1983] as follows:

$$R_L = \frac{0.49\,q^{2/3}}{0.6\,q^{2/3} + \ln(1 + q^{1/3})}, \tag{3.4}$$

for all values of q. In highly-detached D binaries, R_1 and R_2 are both much smaller than R_L. In semi-detached cases, either R_1 or R_2 is near in size to R_L, but not both. If both radii are nearly equal to R_L, the binary is an OC system.

Lastly, the amplitude of the ellipsoidal light variations often seen in an EB light curve outside of the eclipse regions can also be used to study the masses and radii of component stars. These variations are the result of tidal distortions of the star's surfaces, and thus the amplitude of the effect is highly sensitive to the size of the star compared to its respective R_L.

In the case where only one star has a radius that is a significant fraction of its Roche lobe (e.g., as in an SD binary), the amplitude of the ellipsoidal light variations,

A_{elv} is approximately

$$A_{elv} = 1.5 \frac{M_2}{M_1} \left(\frac{R_1}{a}\right)^3, \tag{3.5}$$

where M_1 and R_1 are the mass and radius of the star which is being tidally distorted [Carter et al., 2011]. If both stars have significant tidal distortion (as in something approaching an OC binary), A_{elv} is simply a sum of the previous calculation for each star:

$$A_{elv} = 1.5 \frac{M_2}{M_1} \left(\frac{R_1}{a}\right)^3 + 1.5 \frac{M_1}{M_2} \left(\frac{R_2}{a}\right)^3. \tag{3.6}$$

For example, if each star has a radius of $\sim$10% of the orbital separation, and $q \simeq 1$, then $A_{ELV} \simeq 0.003$. Such an amplitude is easily detectable with Kepler photometry.

3.1.2 Detached Binaries

A detached binary system is one in which the separation between the constituent stars is large relative to their radii [Prša et al., 2011]. In these cases, the duration of the eclipses is relatively short compared to the orbital period, so the dips in the light curve of a D binary are typically narrow. It is usually possible to identify one deep (primary) and one shallow (secondary) eclipse event per orbital period. Exceptions to this rule include systems with substantial eccentricities - in which case only one of the stars may eclipse - and systems in which the constituent stars are equal in size and brightness - in which case the primary and secondary eclipses may be nearly indistinguishable from each other.

Furthermore, because the stars in these systems are usually too separated to tidally deform each other's surfaces, the primary out-of-eclipse variations seen in the light curve of a D binary may be due to stellar oscillations in the component stars themselves. To be exact, A_{ELV} for a system where $q \simeq 1$ will drop below 10^{-5} (approximately the lowest fractional amplitude which *Kepler* can reliably detect) if $R_1/a < 0.02$. While ellipsoidal light variations can still be present, they are typically more noticeable in SD binaries.

The FFT of a D binary light curve is easily recognizable. Typically, the base frequency tends to be lower in a D binary than in the other binary classes (i.e., D

binaries tend to have larger periods). As such, the pattern of harmonics in the FFT is dense. These harmonics often form a broad envelope of peaks at low frequencies as seen in Figures 3-1 and 3-2. Figure 3-2 illustrates both the FFT pattern and phase-folded light curve of KIC 8589731, which we have found and identified as a D binary, and which is not in the Prša catalog.

3.1.3 Semi-Detached Binaries

Prša et al. define an SD binary to be a system in which one component star has filled or nearly filled its Roche lobe while the other remains detached [Prša et al., 2011]. The separation between the stars relative to their radii is thus intermediate between D and OC systems. Eclipses in SD binaries are usually still well-defined, though they are typically wider relative to the orbital period than those of D binaries.

Out-of-eclipse regions in the light curves of SD binaries tend to be rounded as a result of tidal deformations of the surface of one or both component stars. These ellipsoidal light variations differ in amplitude from system to system but are relatively constant within one light curve.

While no pattern in frequency space uniquely identifies an SD system, the FFT of an SD light curve will usually contain a series of peaks at the base frequency and its harmonics. If the two eclipse events are similar in depth and width, the peak at the base frequency and its even-numbered harmonics may nearly disappear, as the system appears to be varying at twice the base frequency, i.e., at the frequency of the first harmonic (see Figure 3-1).

As an example of an SD binary that was identified in this research, KIC 9935242 is examined in Figure 3-3.

3.1.4 Overcontact Binaries

If the two stars of a binary system are so close that they both essentially fill their Roche lobes (i.e., they share a common envelope), they constitute an OC binary [Prša et al., 2011]. In these cases, eclipses are no longer identifiable as sharp dips

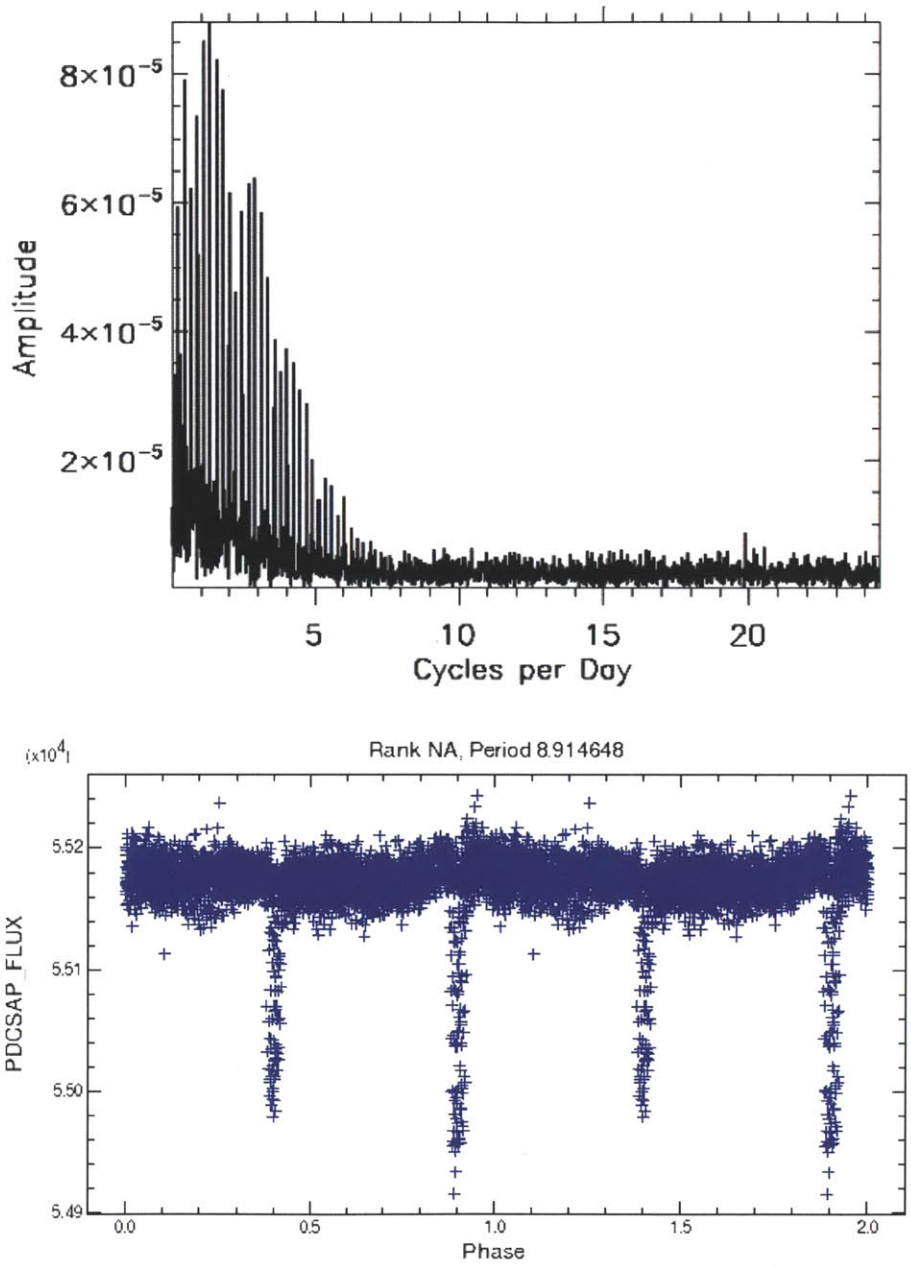

Figure 3-2: The detached binary KIC 8589731. Top: The FFT of the star's light curve, which demonstrates the representative pattern of detached binaries. Bottom: When the light curve is folded about a period of 8.915 days, the primary and secondary eclipses of this system are clearly visible, even though their depth is only one part in 500. The modulation that is seen in the out-of-eclipse region is likely due to sunspots on one or both stars.

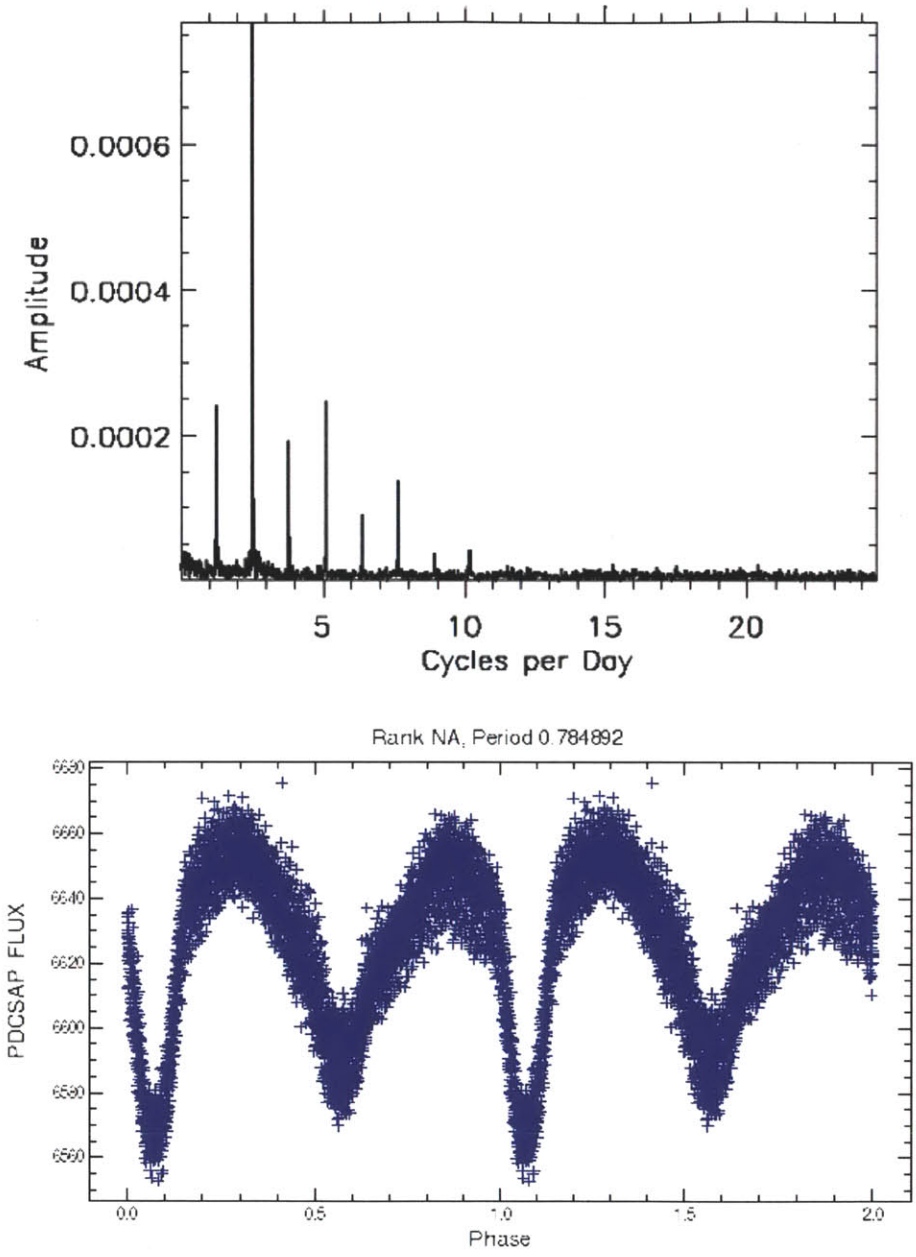

Figure 3-3: The semi-detached binary KIC 9935242. Top: The FFT of the star's light curve, which demonstrates the representative pattern of semi-detached binaries. Bottom: When the light curve is folded about a period of 0.785 days, the primary and secondary eclipses and out-of-eclipse variations are clearly visible.

in flux, as the flux of the system is constantly changing, and no well-defined out-of-eclipse regions exist. When phase-folded at the orbital period, the light curve of an OC system appears to modulate continuously, and there are often two distinct local minima of disparate depths per period (the primary and secondary eclipses).

The FFT of an OC binary can be similar to that of an SD, except that the peak at the base frequency of an OC system is often very low compared to the peak at its first harmonic, and the peaks at the even-numbered harmonics may be nearly nonexistent (see Figure 3-1). KIC 4859432, an OC system not found in the Prša catalog, is shown in Figure 3-4 as representative of this class.

3.1.5 Ellipsoidal Light Variables

All three of the classifications discussed so far are more generally known as eclipsing binaries. But a fourth class of binary in which no eclipses occur can also be identified photometrically. If the components of a binary are near enough to distort each other's surface, but the inclination of the orbital plane is such that neither star passes between its companion and the observer, it is still possible to detect changes in brightness due to the changing cross-sections and surface gravities of each star [Prša et al., 2011]. The light curves of these ellipsoidal light variation (ELV) systems are near-sinusoids with no detectable eclipse events and a dominant period at twice the orbital frequency. As such their FFTs usually show little more than a single tall peak at the first harmonic of the base frequency, and perhaps small peaks at the base frequency and its second harmonic (see Figure 3-1). Figure 3-5 shows KIC 7900367, an example of this class which was discovered in this work.

3.2 RR Lyrae Stars

The variable star RR Lyrae is located near the boundary between the Lyra and Cygnus constellations, fortuitously placing it within *Kepler*'s field of view. RR Lyrae serves as the archetype of a class of low-mass pulsating stars which are late in their evolutionary lives [Nemec et al., 2011], burning He in their cores after descending

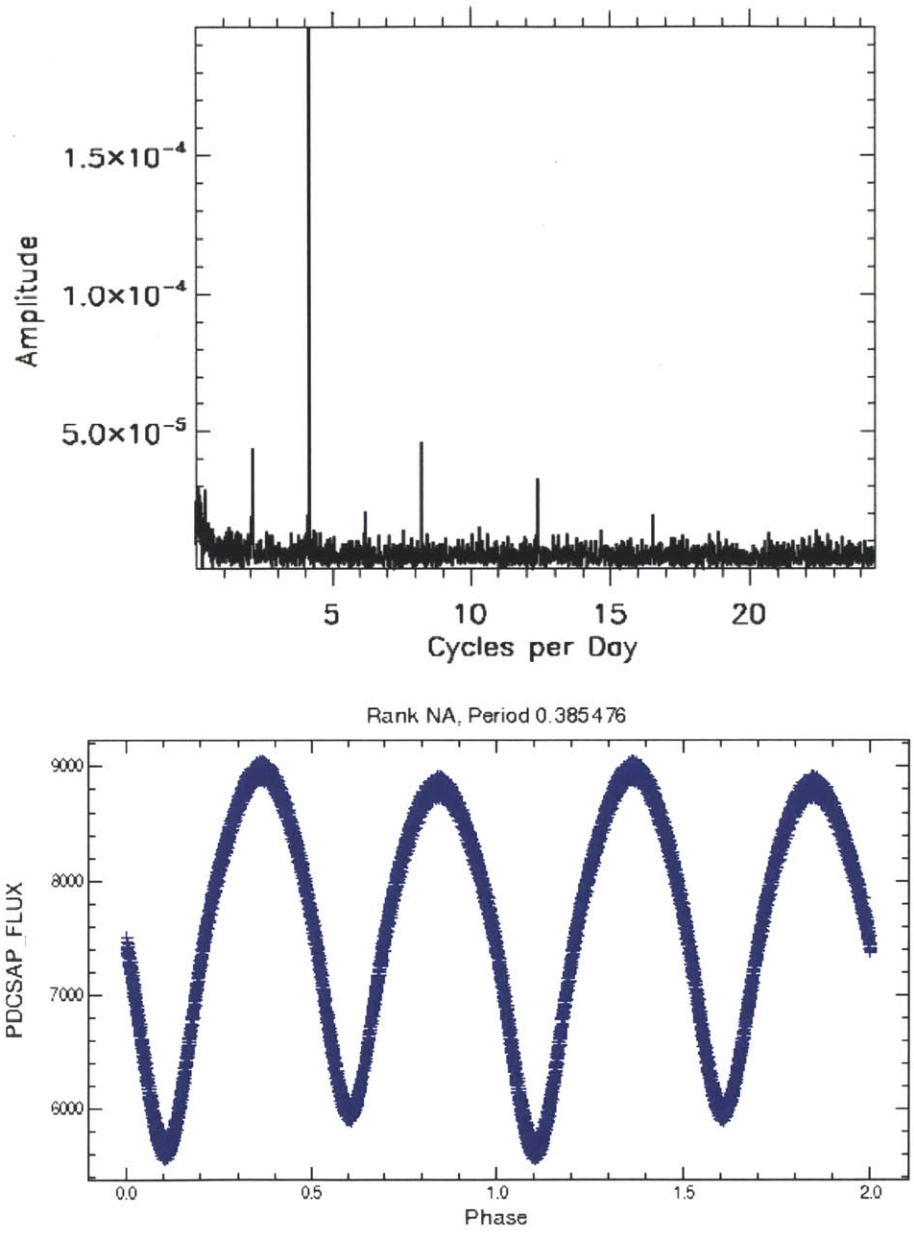

Figure 3-4: The overcontact binary KIC 4859432. Top: The FFT of the star's light curve, which demonstrates the representative pattern of eclipsing binaries. Bottom: when the light curve is folded about a period of 0.385 days, the near-sinusoidal variation of the over-contact system is evident.

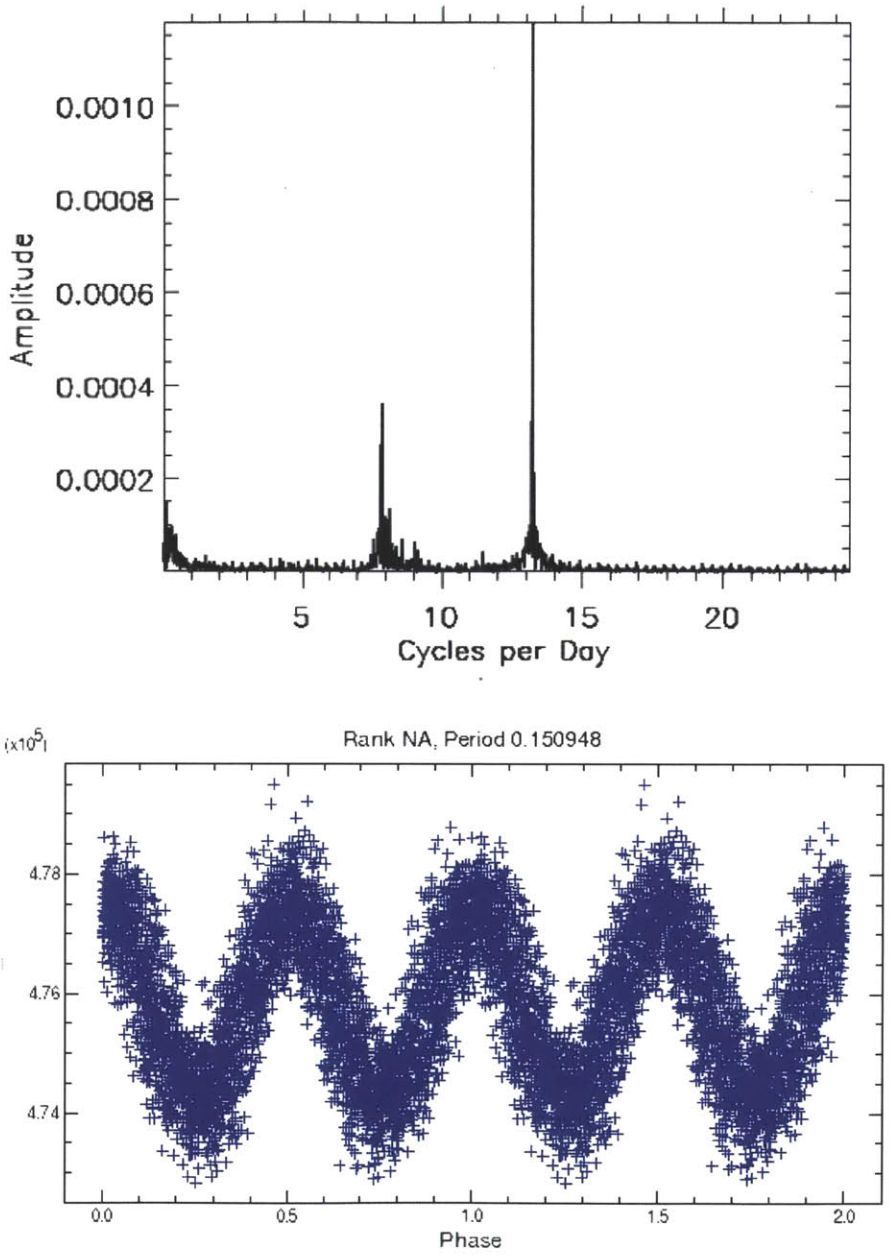

Figure 3-5: The ELV binary KIC 7900367. Top: The FFT of the star's light curve, which contains only two significant peaks, one at the base frequency and a larger one at its first harmonic. Bottom: Phase-folding the light curve at twice the system's orbital frequency produces this sharp-featured, nearly sinusoidal curve, which is representative of ELV binaries.

from their first ascent of the giant branch. As shown in the work by Nemec et al., these stars are useful to the study of stellar evolution, and efforts to catalog their numbers in the *Kepler* FOV (estimated to be ≈ 80) have been ongoing since 2010 [Kolenberg et al., 2010].

Over the course of one pulsation cycle, the brightness of an RR Lyrae type star will dip slightly, then rise quickly and dramatically (by a whole magnitude), and finally gradually fall to quiescent levels [Kolenberg et al., 2010]. This periodic brightening effect makes the stars readily identifiable.

Since the FFTs of RR Lyrae stars follow nearly the same pattern as D and SD systems, it is easy to mistake these stars for binaries until phase-folds reveal their distinctive shape and very large amplitudes. We offer a catalog of the RR Lyrae stars we found during this research in Appendix C. Figure 3-6 gives the FFT and phase-fold of KIC 6763132, a clear RR Lyrae star.

3.3 Sub-Giants with Solar-Like Oscillations

Our early studies of the candidates which passed the FFT selection algorithm revealed a commonly recurring pattern in approximately 200 of the $4,674$ candidates. The FFTs of these light curves have an overall envelope shape similar to f^{-1}, where f is the frequency of oscillation, except with the addition of a significant cluster of peaks usually between 5 and 10 oscillations per day.

Further research found these features were characteristic of sub-giant or red giant stars which are undergoing solar-like oscillations. These oscillations provide direct information on the mean densities and surface gravities of these stars, from which one can infer their masses and radii. Considerable research on the phenomena within the *Kepler* database has already been conducted [Hekker et al., 2011]. An example of the FFT patterns of these sub-giants is provided below. Due to the large number of such cases present in the data and the thoroughness of recent research by the *Kepler* team, we did not attempt to catalog these objects. Figure 3-7 shows the FFT pattern representative of these systems using KIC 1027337 and KIC 9873127 as examples.

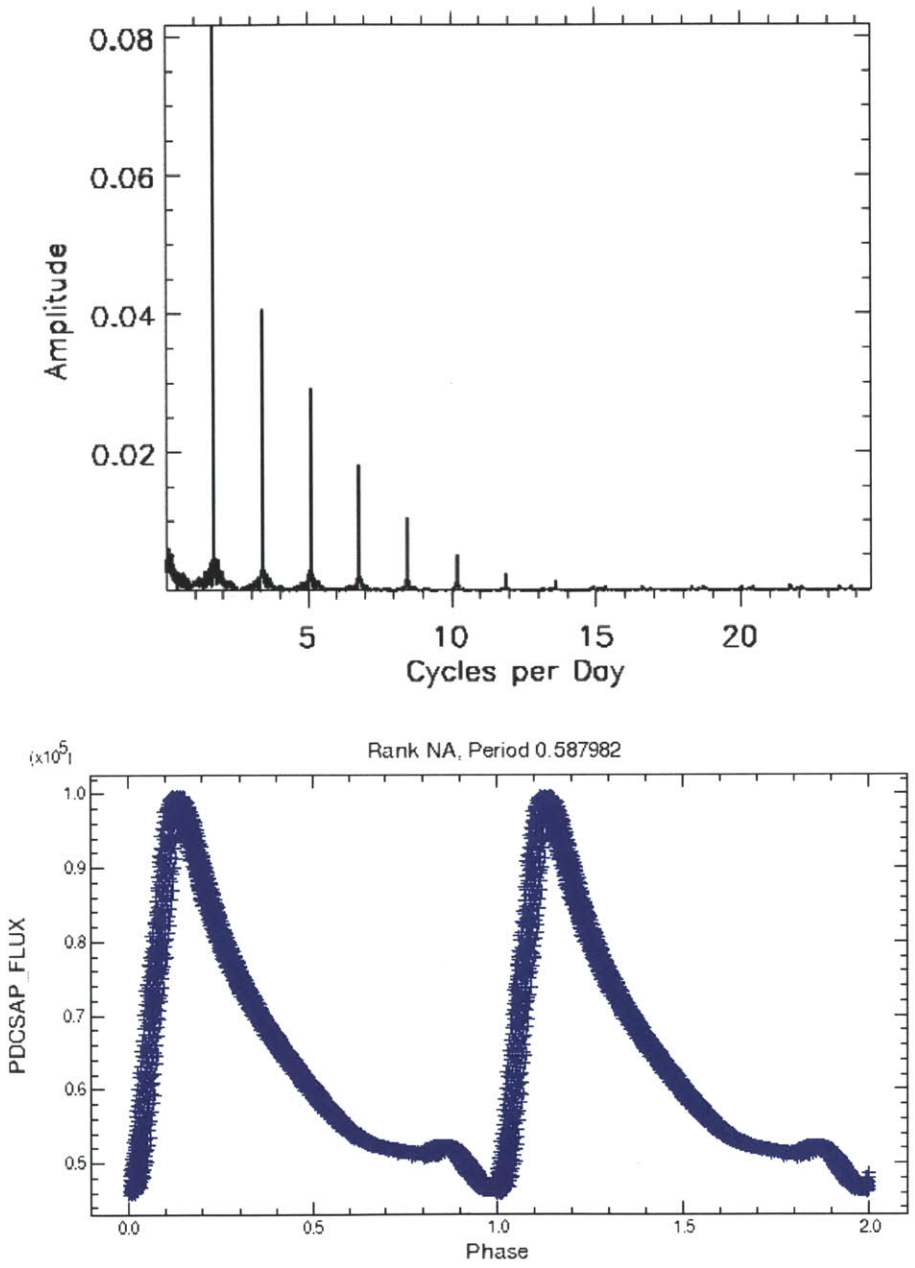

Figure 3-6: The RR Lyrae type of pulsating star KIC 6763132. Top: The equally spaced pattern of significant peaks in this FFT are reminiscent of D or SD binaries, making it easy to mistake RR Lyrae stars for EBs given only this information. Bottom: When phase-folded about the period of pulsation, the short dips followed by sudden and dramatic rises in brightness of an RR Lyrae star are very distinctive.

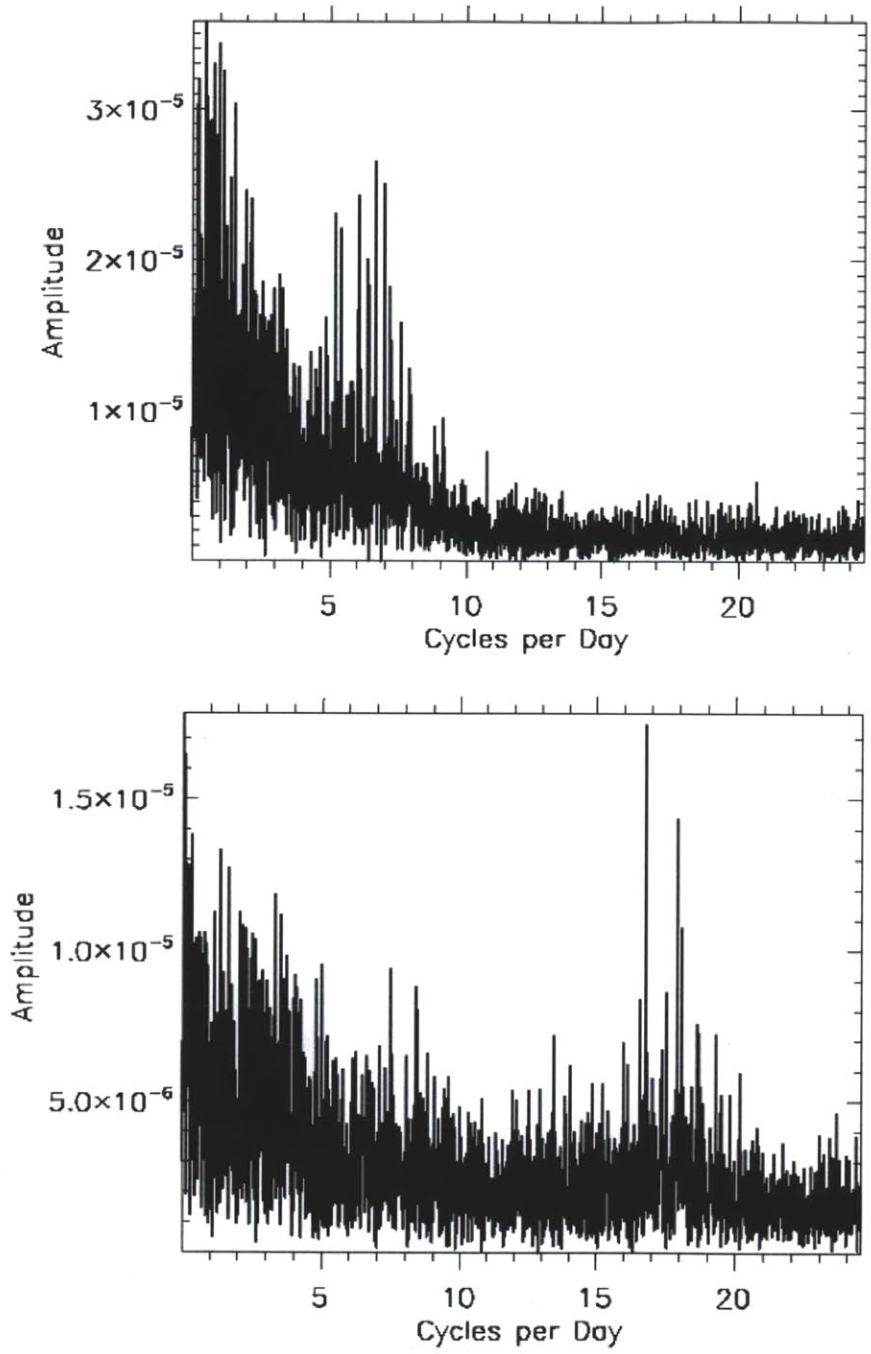

Figure 3-7: Example FFTs of sub-giant pulsators. Top: KIC 1027337 follows the $1/f$ envelope expected of these sub-giants with solar-like oscillations, with a cluster of peaks near 6 cycles/day. Bottom: KIC 9873127 is a similar sub-giant, but with its cluster of peaks appearing at a much higher frequency, near 18 cycles/day.

Appendix A

The Catalog of New Eclipsing Binaries in the *Kepler* Database

Here we present the primary product of this thesis, a catalog of 173 proposed binary systems which were discovered in the *Kepler* database, but which were not found in the *Kepler* team's catalog of binaries [Slawson et al., 2011]. Figure A-1 shows how these systems were distributed by orbital period.

For each system, we provide the identifying Kepler Input Catalog (KIC) number, the orbital period (in days) as determined via phase-fold, the tentative binary classification, the effective temperature (in Kelvin), the logarithm of surface gravity (in cgs units), and the radius (with $R_{\odot} = 1$).

The binary classifications include detached (D), semi-detached (SD), overcontact (OC), and ellipsoidal light variable (ELC), which are explained in detail in Chapter 3. Borderline cases are labelled with the author's best attempt at a proper classification followed by question marks. A system labelled "SD ??" is therefore thought to be semi-detached, but the light curve and FFT stray too far from the SD prototype for this classification to be certain. Another eleven systems which exhibit clear periodic behavior, but could not be classified certainly as binary or any known type of pulsator, are labelled only with question marks and appended to the end of this table.

All values of TEFF, LOGG, and RADIUS are taken from the headers of the target's FITS file, as explained in Chapter 2.

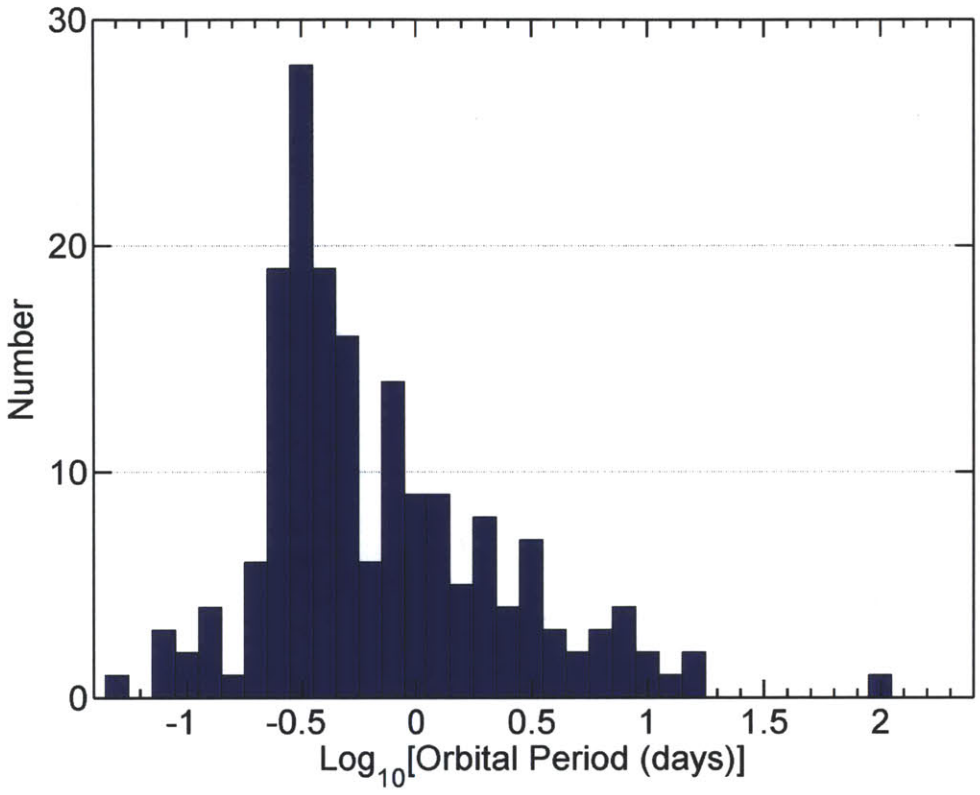

Figure A-1: The distribution among orbital periods of the *Kepler* targets classified as "new" binaries by this research.

Table A.1: Catalog of Eclipsing Binaries

KIC	PERIOD	CLASS	TEFF	LOGG	RADIUS
1867844	0.350654	SD	0	0	0
2019076	7.132092	D	5624	4.454	1.01
2300319	0.282018	ELV	0	0	0
2451721	0.356906	ELV	6123	4.426	1.068
2719436	0.743464	SD	7041	4.117	1.64
2851278	0.21927	SD	6482	4.147	1.537
3114661	0.888684	D	5096	4.722	0.682
3124412	0.948955	SD	6016	4.409	1.087
3232859	8.387211	D	6020	4.454	1.028
3337351	14.09423	D	0	0	0
3338674	1.873112	SD	4711	2.75	8.398
3344419	0.651782	SD	5348	4.379	1.084
3356010	0.410586	OC	5393	4.478	0.961
3442058	1.429642	ELV	7487	3.954	2.085
3533195	0.448112	SD	6238	4.195	1.431
3542222	0.50444	SD	5790	4.452	1.02
3549993	0.34718	SD	5423	4.829	0.617
3560212	0.346064	SD	5233	4.501	0.919
3648131	0.129746	OC	7475	3.951	2.09
3655332	15.066423	D	5549	4.419	1.047
3735634	9.33768	D	5900	4.188	1.424
3868420	0.416472	ELV ??	6565	4.051	1.745
3965879	0.30592	ELV	6269	4.298	1.257
4037164	0.635445	SD	3900	4.564	0.616
4070633	0.417656	OC	4108	4.544	0.678
4241946	0.28438	OC	4663	4.469	0.881
4364460	0.680138	OC	5498	4.363	1.118

KIC	PERIOD	CLASS	TEFF	LOGG	RADIUS
4377638	2.820992	SD	9093	3.884	2.631
4446411	1.256312	SD	5462	4.39	1.078
4464528	0.219142	SD	6088	3.887	2.118
4474916	0.34568	OC	6010	4.248	1.323
4476900	0.279664	OC	5222	4.525	0.891
4579313	2.11176	D	5363	4.666	0.755
4678875	1.88012	D	6259	4.266	1.309
4843592	0.483516	SD ??	5499	4.395	1.075
4859432	0.385476	OC	5067	4.494	0.913
5022916	0.244526	ELV ??	5068	4.642	0.754
5041847	0.457254	SD	5538	4.417	1.049
5174346	0.350598	OC	5726	4.396	1.09
5197256	6.95825	SD	7609	3.879	2.321
5220019	0.363972	ELV	4731	4.545	0.803
5355850	0.106642	ELV ??	8135	3.603	3.485
5390342	0.547554	SD	6275	4.673	0.795
5436161	0.64422	SD	5001	4.452	0.958
5467126	2.845052	D	4683	2.522	10.878
5471606	0.962746	D	0	0	0
5473826	1.054944	SD	10927	4.129	2.216
5513866	1.510646	SD ??	0	0	0
5535890	3.252704	SD	5911	4.356	1.154
5543482	0.29482	OC	5156	4.578	0.827
5560830	0.867396	SD	5954	4.401	1.093
5563614	0.372252	ELV ??	5823	4.064	1.669
5565497	0.94158	D	8314	4.023	2.042
5597891	0.494192	OC ??	0	0	0
5611561	0.258696	OC	0	0	0
5816811	4.455431	D	5768	4.528	0.928

KIC	PERIOD	CLASS	TEFF	LOGG	RADIUS
5891611	0.281236	OC ??	5220	4.495	0.925
5956051	0.89284	OC ??	4691	4.543	0.798
5977736	1.578218	OC ??	7661	3.809	2.556
5979800	0.743334	SD	5032	3.772	2.409
6045250	0.909268	D ??	6142	4.678	0.785
6045511	0.547162	ELV ??	0	0	0
6148974	0.337808	SD ??	4677	4.558	0.779
6182849	6.40458	D	5893	4.436	1.045
6206125	3.600774	OC ??	8943	4.102	1.95
6231538	0.081463	ELV ??	6488	3.699	2.755
6233483	15.8632	D	5942	4.271	1.282
6267702	0.283196	ELV	5065	4.297	1.178
6267702	0.283196	OC ??	5065	4.297	1.178
6311681	0.844784	SD	5500	4.453	1.001
6312534	1.00505	D	4897	4.521	0.858
6314185	1.433122	D	5709	4.328	1.183
6470521	2.07975	D	6185	4.396	1.111
6599775	0.53529	SD ??	5762	4.449	1.023
6633929	0.358926	OC	5482	4.413	1.05
6665064	0.698392	SD	5780	4.33	1.185
6669790	0.733798	SD	5676	4.424	1.049
6677267	3.126944	D	5852	4.353	1.155
6947064	0.087754	OC ??	8172	3.913	2.327
7022707	0.311744	SD	5871	4.429	1.052
7025526	2.148162	D	4662	4.412	0.954
7117514	0.290388	SD	5855	4.595	0.858
7198474	0.242324	SD ??	5759	4.659	0.789
7220322	0.752163	SD	0	0	0
7376490	2.93882	D	5548	4.318	1.186

KIC	PERIOD	CLASS	TEFF	LOGG	RADIUS
7385509	3.310946	SD	0	0	0
7418173	0.780712	SD	5146	3.767	2.444
7432476	0.40848	OC	5058	4.898	0.54
7440742	0.283992	OC	4834	3.615	2.959
7516354	0.491722	SD ??	5073	2.584	10.222
7530366	0.52557	SD ??	9486	3.537	4.266
7707736	0.758404	D	5435	4.799	0.643
7732791	2.064284	D	4197	4.54	0.703
7740566	0.297072	OC	5526	4.422	1.041
7777435	0.09893	OC ??	8122	3.75	2.87
7800087	0.0472088	ELV ??	3828	4.358	0.843
7825764	0.275514	ELV ??	5636	4.403	1.076
7833144	2.24086	ELV ??	7724	3.613	3.325
7848288	0.130862	ELV ??	7384	3.519	3.668
7900367	0.150948	ELV	6972	4.14	1.587
8028158	0.271036	ELV ??	5484	4.525	0.913
8038679	2.22081	ELV	7168	4.035	1.835
8097553	0.391228	OC	5408	4.44	1.009
8097897	0.331548	OC	5469	5.096	0.44
8120272	2.487758	OC ??	5268	4.131	1.493
8211618	0.337452	OC	5556	4.426	1.038
8211824	0.841064	D ??	4860	4.547	0.822
8263752	3.664552	D	6320	4.358	1.171
8555795	0.234524	SD	5002	4.758	0.543
8589731	8.914648	D	5529	3.801	2.337
8620565	0.782044	D	5838	4.455	1.018
8682132	0.300572	SD ??	5940	4.791	0.675
8694926	0.37149	OC	5583	4.44	1.024
8757910	1.310006	D	6163	4.408	1.094

KIC	PERIOD	CLASS	TEFF	LOGG	RADIUS
8780959	5.247132	D	6210	4.19	1.438
8782626	0.307908	OC ??	6090	3.709	2.679
8845312	0.319816	ELV	7305	3.412	4.191
8937021	5.663653	D	4764	4.597	0.753
9075708	0.513164	SD	3986	4.521	0.676
9097892	1.674868	D	6142	4.337	1.192
9282769	1.33275	D	6138	4.277	1.283
9329214	0.281502	ELV ??	5852	4.431	1.05
9392331	0.261764	OC	5993	4.524	0.943
9450883	0.363666	OC ??	5755	4.381	1.11
9456932	1.053708	OC	5620	4.493	0.962
9520019	0.599724	SD ??	5152	4.457	0.965
9535881	0.480494	SD	7173	4.182	1.521
9651298	2.15686	OC	7677	3.732	2.832
9653378	0.39529	ELV	5453	4.358	1.122
9664387	0.290756	OC	6153	4.591	0.875
9665086	0.296536	SD	0	0	0
9703626	0.415144	OC	6163	4.493	0.986
9773512	0.217222	ELV ??	7956	3.701	3.012
9773512	0.217222	ELV ??	7956	3.701	3.012
9774314	0.1123	ELV ??	7903	4.011	1.997
9774314	0.1123	ELV ??	7903	4.011	1.997
9776718	0.544348	OC	0	0	0
9834257	1.304492	D	6342	4.189	1.449
9851142	8.47987	D	6804	3.947	2.014
9892471	8.267872	D	5496	4.509	0.933
9935242	0.785212	SD	5752	4.461	1.006
9935242	0.785212	SD	5752	4.461	1.006
10020247	0.345536	OC	5439	4.848	0.604

KIC	PERIOD	CLASS	TEFF	LOGG	RADIUS
10074939	0.277096	OC	4812	4.717	0.651
10322287	0.31503	ELV ??	3849	4.496	0.678
10451317	2.27677	ELV ??	7048	4.026	1.841
10488450	5.366772	D	0	0	0
10489525	3.224042	D	6478	3.866	2.208
10549643	0.086402	OC ??	7550	3.991	1.996
10596883	0.468904	OC	7296	4.098	1.709
10737574	0.365664	OC	5510	4.448	1.007
10802917	0.272458	OC	4937	4.505	0.883
10848807	0.346248	OC	5869	4.478	0.992
10879208	1.336968	D	5375	4.623	0.799
10919564	0.462072	SD	5474	4.556	0.878
10932440	0.274076	OC ??	5063	4.405	1.024
11151677	0.360224	SD	6078	4.453	1.032
11352791	0.28052	OC	6059	4.424	1.068
11403776	0.401812	SD	5571	4.529	0.916
11599937	0.262208	SD	5626	4.716	0.728
11671429	112	D	7363	3.578	3.388
11710139	0.340834	OC	5359	4.476	0.96
11811382	0.265328	OC	5249	4.378	1.076
11817498	0.384432	ELV ??	5879	4.677	0.775
11820830	1.21281	D	7007	4.224	1.428
11825056	0.532012	SD	5854	4.388	1.107
11904306	1.393308	ELV	0	0	0
12071598	0.230364	SD	4711	4.688	0.661
12350008	0.184532	SD	6108	4.634	0.827
12366948	0.280384	SD	6065	4.447	1.038
12367017	1.221862	D	5004	4.348	1.097
12404615	0.366304	OC	0	0	0

KIC	PERIOD	CLASS	TEFF	LOGG	RADIUS
12508348	0.255618	ELV	8961	4.037	2.129

Appendix B

A Catalog of RR Lyrae Stars Found in the *Kepler* Database

This catalog contains 24 RR Lyrae systems which were found during this study. The dramatic modulation in brightness seen in these stars (often on the scale of one whole magnitude magnitude) could cause background contamination in other *Kepler* targets. As such, this list is provided to facilitate the identification of false-positives.

The labels for each column are the same as those in Appendix A, except the "Class" of each system is simply "RR Lyrae". Figure B-1 shows how these objects are distributed by pulsation period.

Table B.1: Catalog of RR Lyrae Systems

KIC	PERIOD	TEFF	LOGG	RADIUS
3733346	0.682118	6424	3.903	2.099
3866709	0.470714	8452	3.966	2.231
5299596	0.523548	5424	3.646	2.862
5559631	0.620724	5884	3.996	1.827
6070714	0.5342	6319	4.24	1.355
6100702	0.488194	6693	4.079	1.694
6183128	0.561714	0	0	0

KIC	PERIOD	TEFF	LOGG	RADIUS
6763132	0.587982	7797	3.775	2.699
7021124	0.622352	0	0	0
7030715	0.684304	0	0	0
7176080	0.507096	6270	4.276	1.292
7198959	0.56682	0	0	0
7295372	0.535441	6221	4.209	1.403
7505345	0.473708	7775	3.765	2.732
7671081	0.504425	7126	4.07	1.749
7742534	0.456568	8477	3.894	2.457
7988343	0.581076	6087	3.979	1.879
8344381	0.577012	7968	4.075	1.846
9001926	0.556986	7315	4.124	1.656
9508655	0.594202	7308	4.014	1.904
9947026	0.549062	7428	3.881	2.282
9947026	0.549062	7428	3.881	2.282
10136240	0.56588	0	0	0
10136240	0.56588	0	0	0
10789273	0.48028	8345	3.85	2.569
11125706	0.613364	0	0	0
12155928	0.436442	6770	4.095	1.666

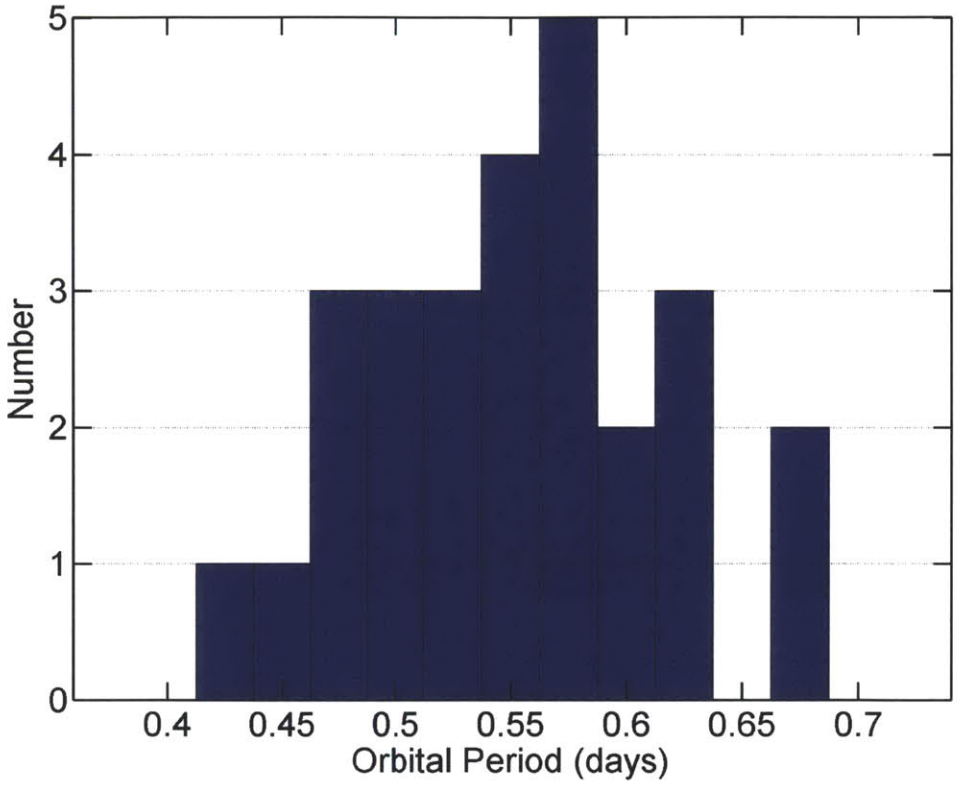

Figure B-1: The distribution among pulsation periods of the RR Lyrae type stars found in this research. Note that the range of this distribution is less than 0.3 days.

Appendix C

Other Objects of Interest

In this appendix we provide some additional figures for two categories of objects. The first set of figures (Figure C-1 to Figure C-4) is meant to expand upon Chapter 3 by providing three additional examples of detached binaries and a single additional example of a semi-detached binary. All four additional examples contain interesting features explained in the figure captions.

The second group of objects were encountered during this study and might be categorized as "peculiar objects" for the following reasons:

- KIC 11671429 is a D binary with the second longest orbital period of the *Kepler* binaries at ~112 days (Figure C-5).

- KIC 8759967 fluctuates oddly in brightness and has been exceedingly difficult to classify. Note, the amplitude of the third harmonic is higher than those of the base frequency and the first two harmonics (Figure C-6).

- KIC 7740983 displays fluctuations which occur at three unique periods, though the causes of the fluctuations are still unknown (Figure C-7).

- KIC 12557548 has been the subject of careful study by our team and seems to be a planetary system in which the planet is disintegrating via the emission of dust (Figure C-8).

Many other objects of interest were discovered in this research, but these four are presented as especially unique cases which could merit further study.

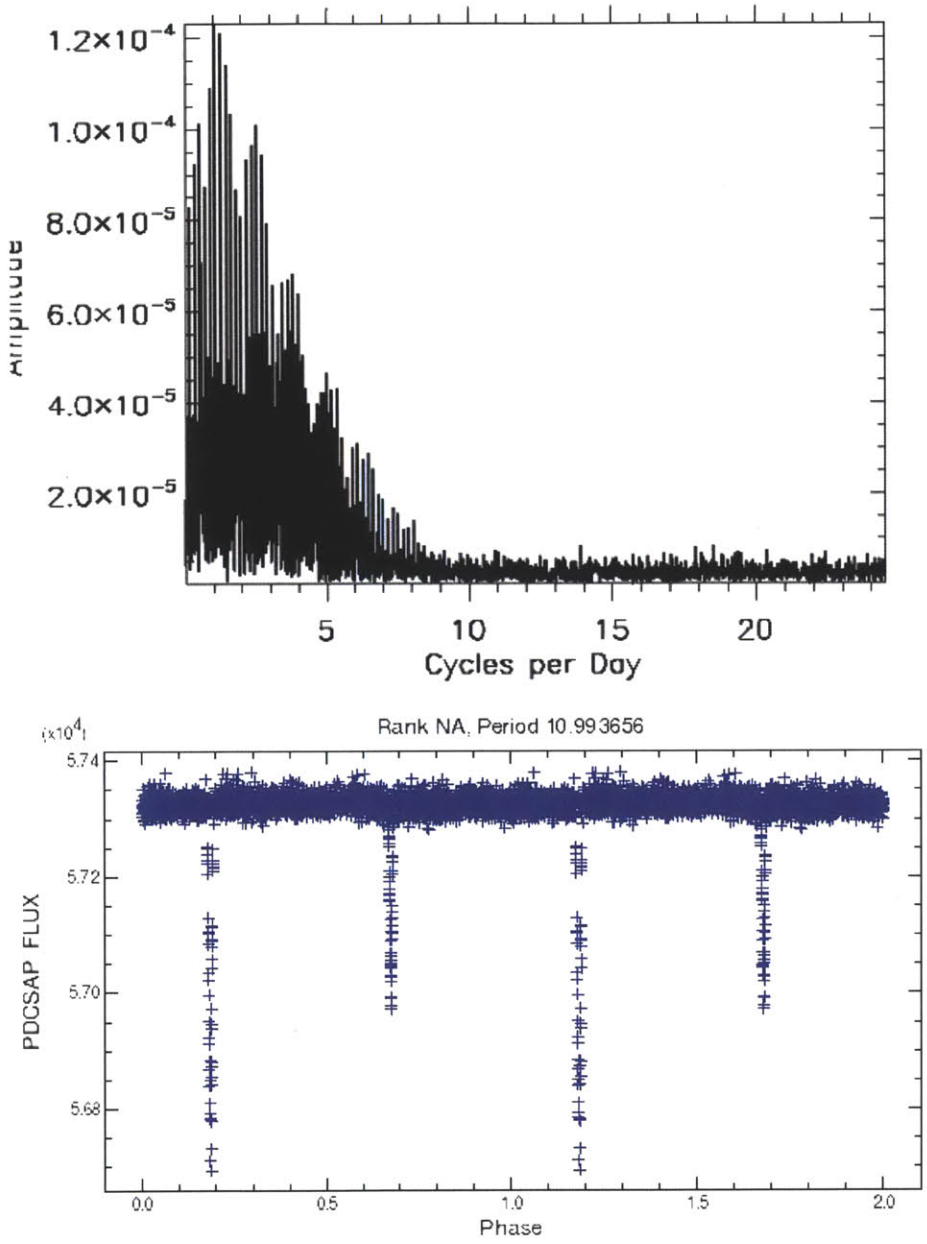

Figure C-1: KIC 8263752. An additional example of a D binary, the orbital period of which (∼10.994 days) is much longer than the duration of its eclipses.

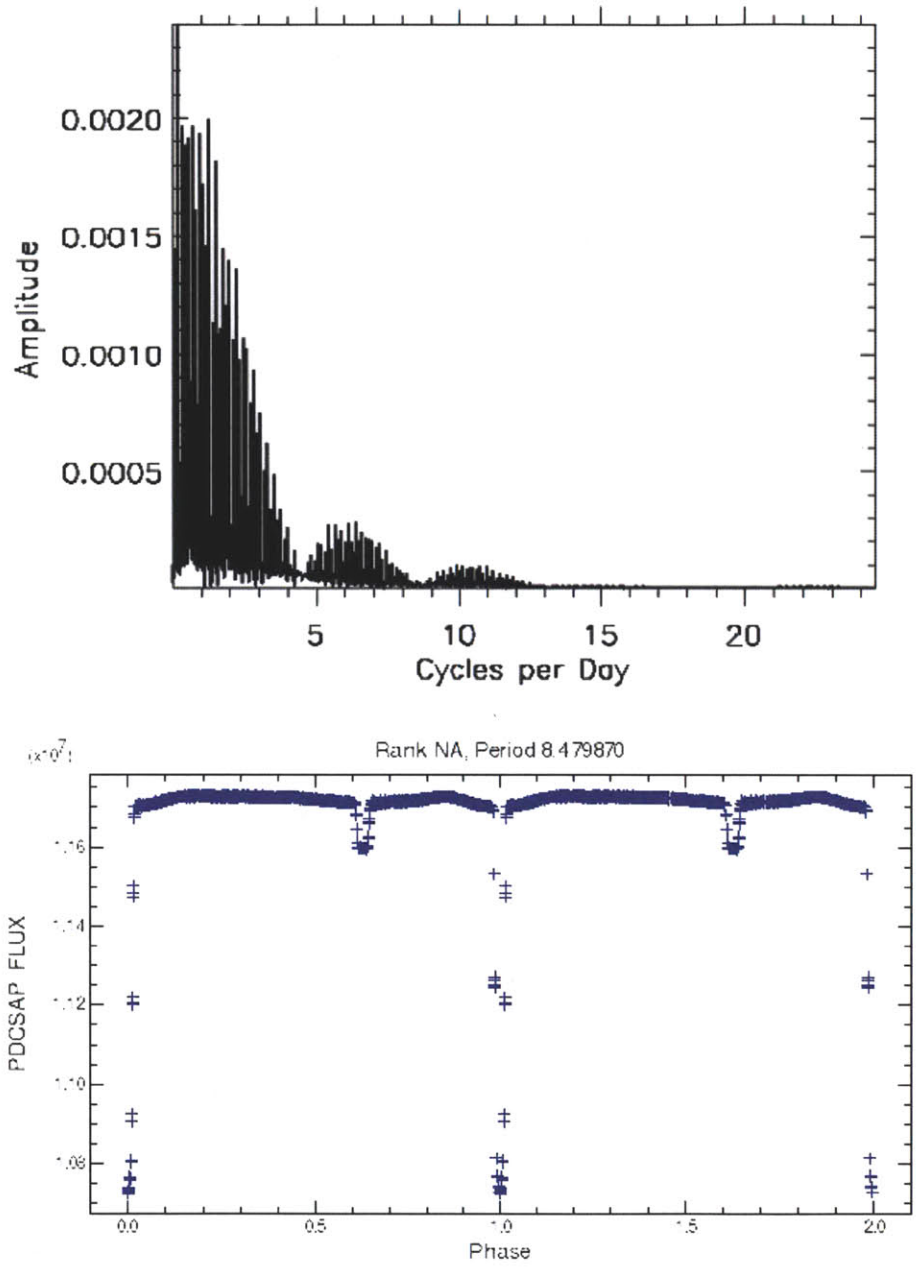

Figure C-2: KIC 9851142. Another D binary, but of particular note because of its flat-bottomed secondary eclipse and clear orbital eccentricity. The secondary star of this system is hypothesized to be a low-mass M or K star.

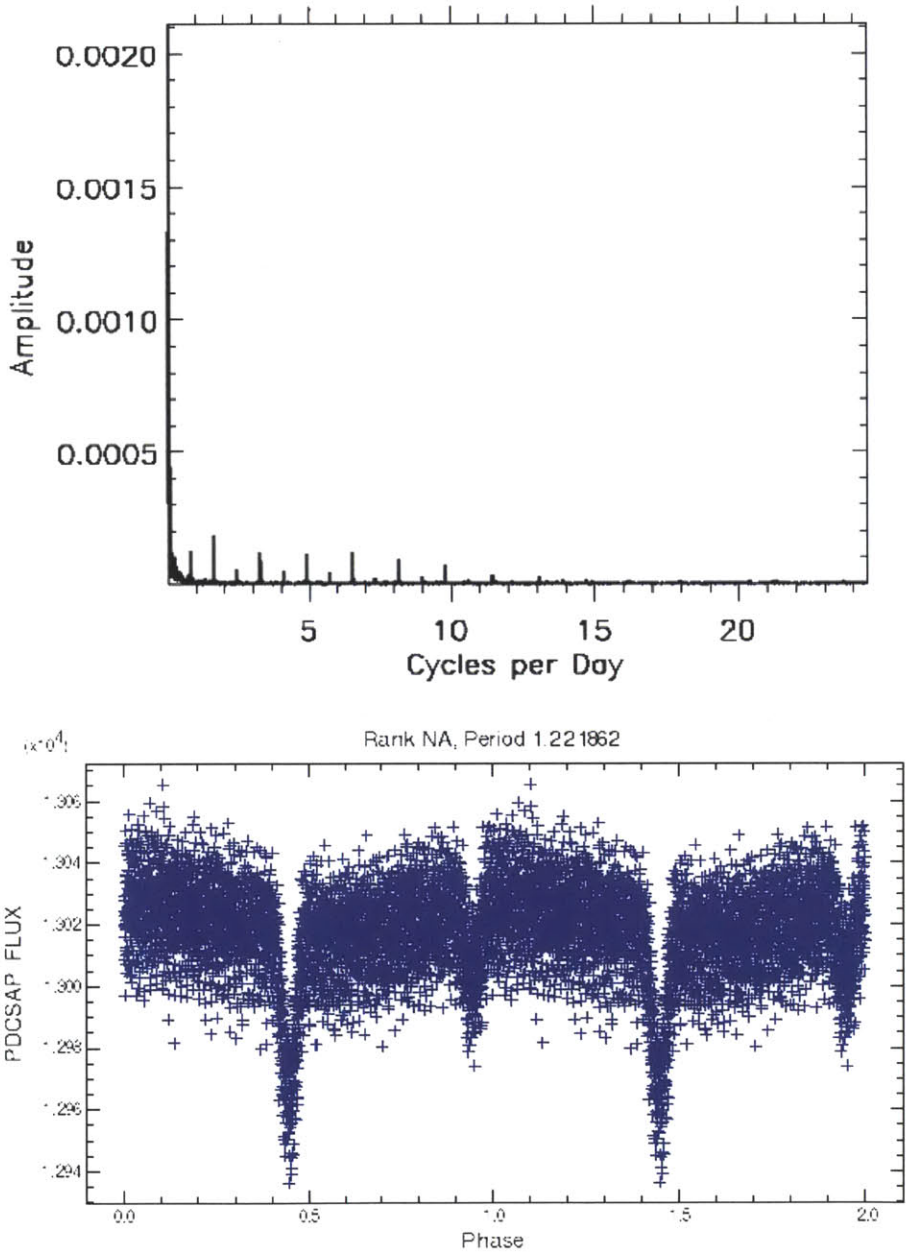

Figure C-3: KIC 12367017. A third D binary, the eclipses of which have relatively small amplitudes when compared to the out-of-eclipse sunspot variation and S/N levels.

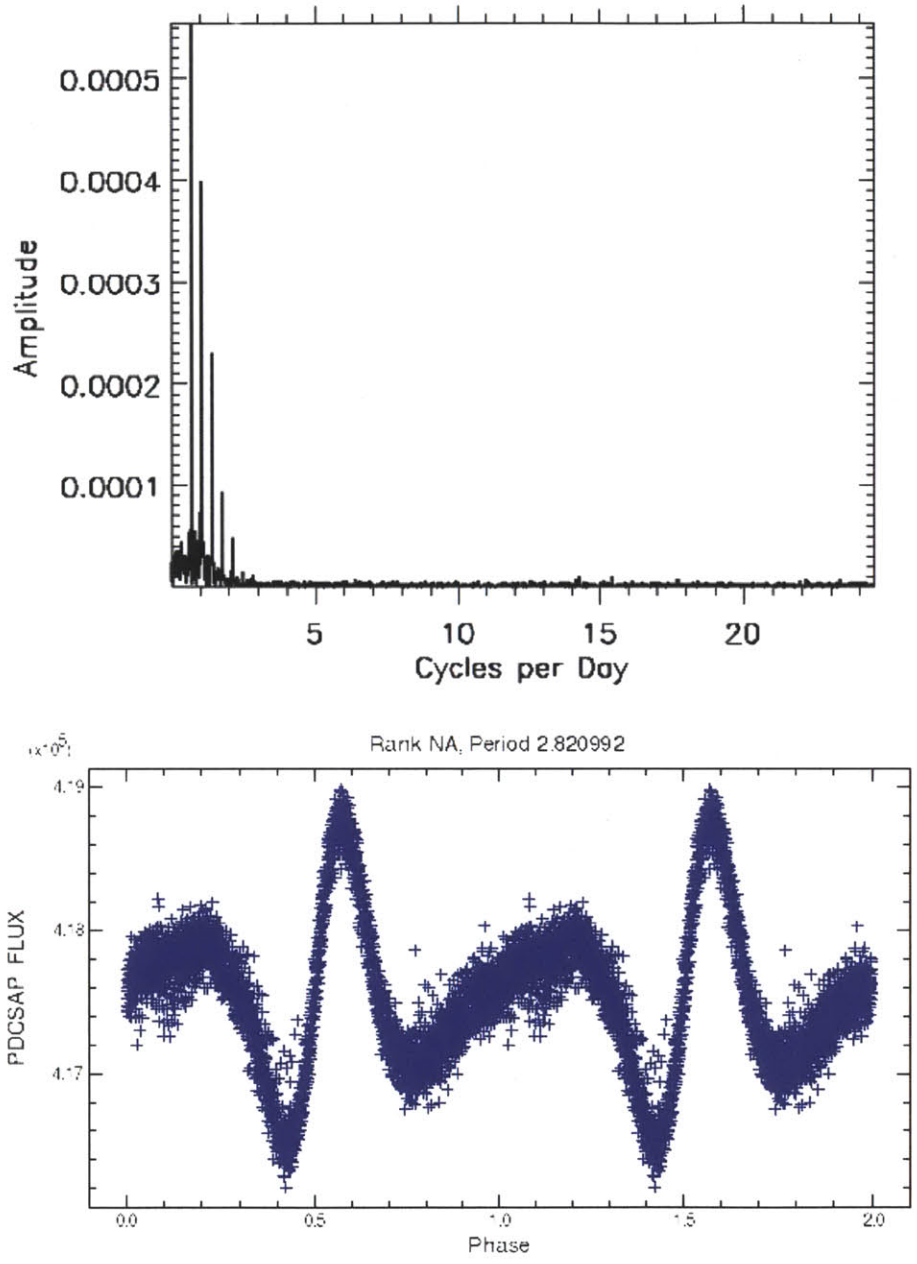

Figure C-4: KIC 4377638. An example of an eccentric SD system with large ELV amplitudes.

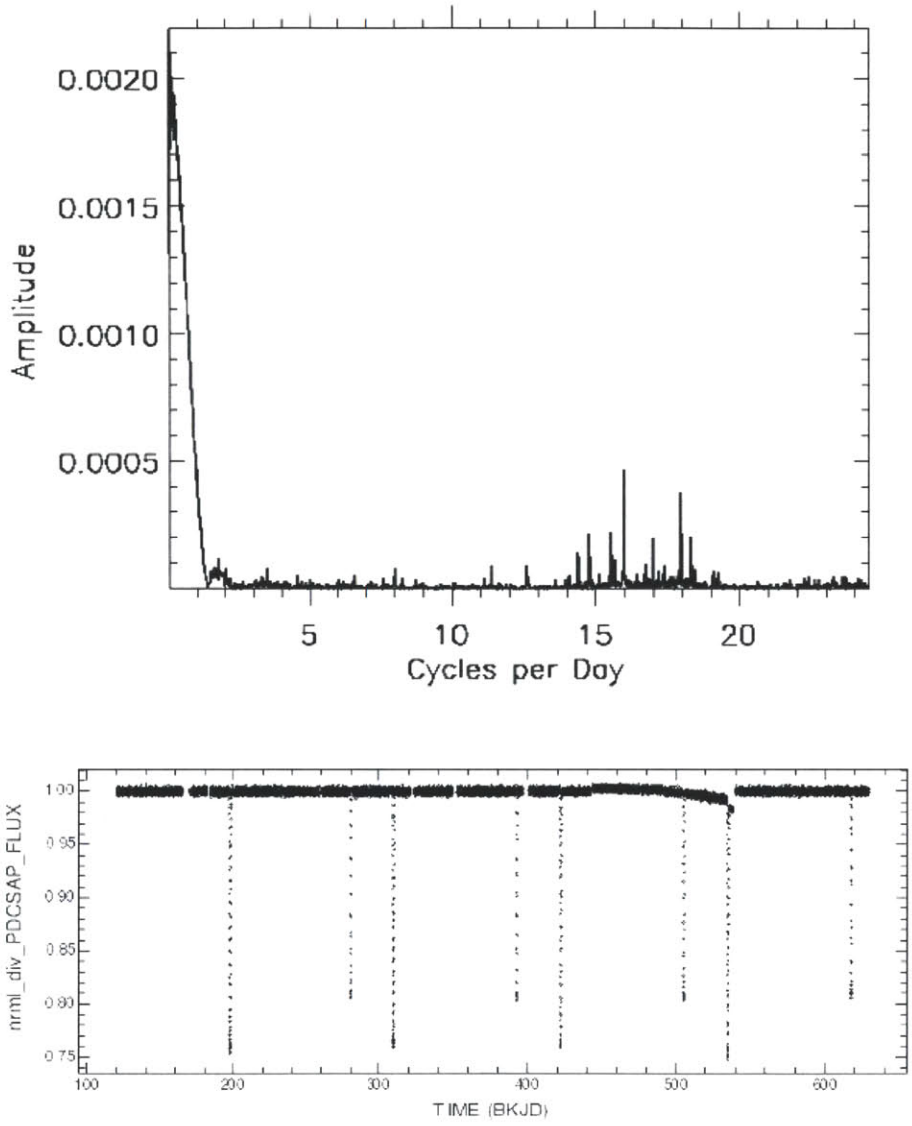

Figure C-5: KIC 11671429. This is a D binary with an orbital period of $\sim$112 days. Only one eclipse was visible in the Q2 data, so multiple quarters had to be concatenated to fully study this object Were it included, this would be the second longest orbital period of all the binaries in the Prša et al. catalog.

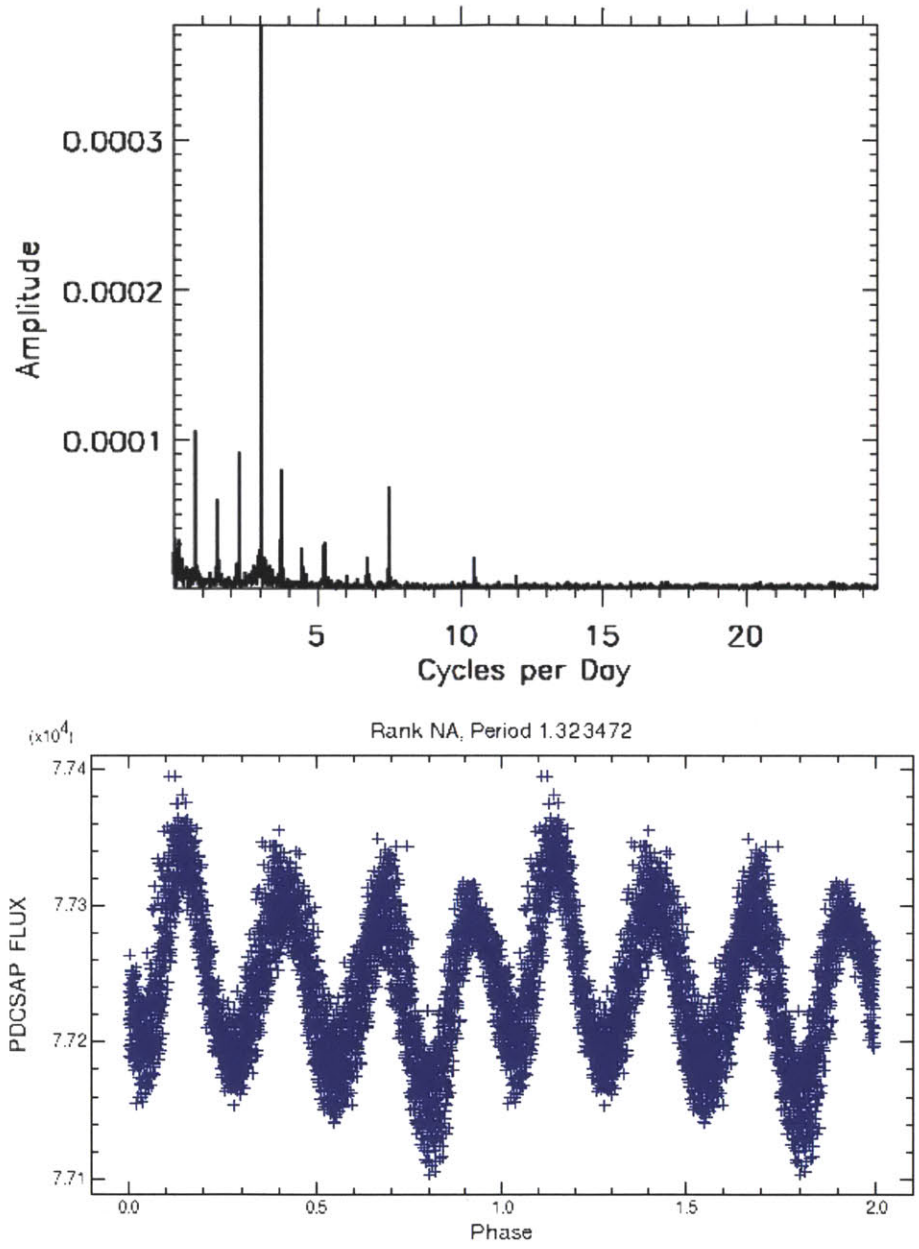

Figure C-6: KIC 8759967. This strange "double-M" object has a light curve with a very odd modulation pattern and has been exceedingly difficult to classify. It could be a pulsator or a binary, but no certain label can be assigned without further observation.

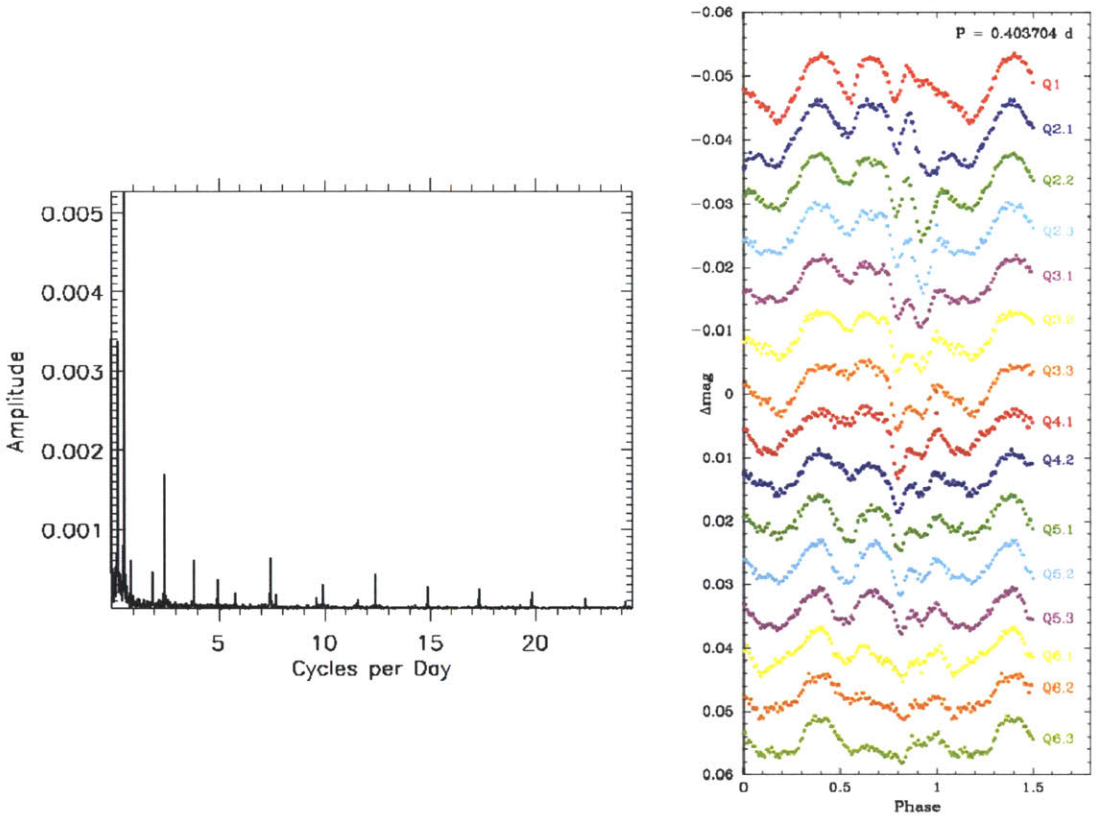

Figure C-7: KIC 7740983. Careful inspection of the FFT (left) reveals three separate base frequencies, each with a corresponding set of harmonics. We have determined that the three independent periods are 3.36, 0.403, and 0.519 days. Spectroscopic observations suggest the target is a low-mass M star, but whether the modulations are due to pulsations or eclipses is still uncertain. The sequence of phase-folds (right) was prepared by Gerald Handler of the Copernicus Astronomical Center.

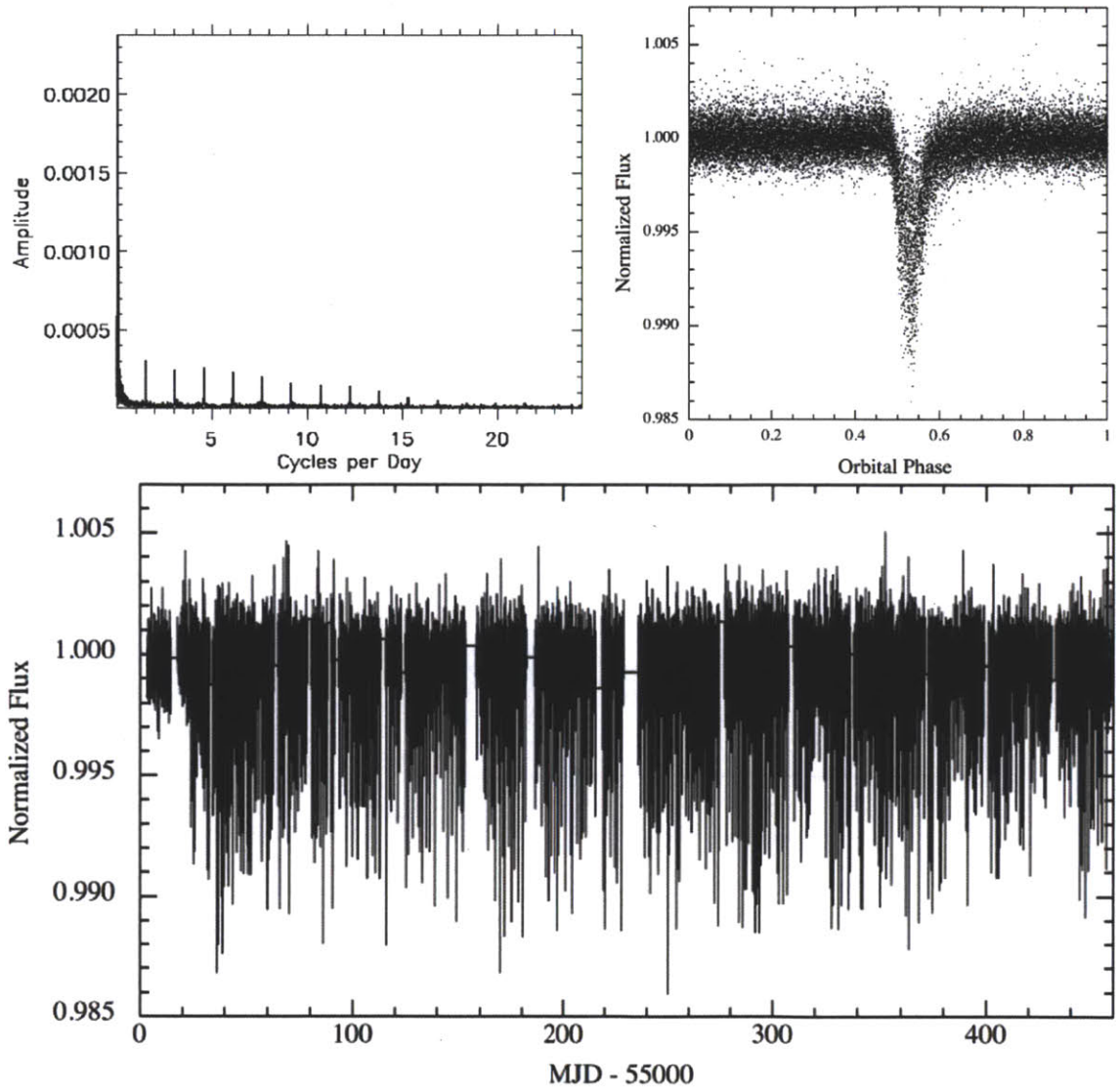

Figure C-8: KIC 12557548. This object was discovered via the FFT selection algorithm and has been extensively reviewed by our team. Eclipses which vary in depth occur every 15.685 hours, and we hypothesize the cause of these events to be the occultation a super-mercury planet which is evaporating via dust [Rappaport et al., in press]. Clockwise from the top left, these plots show (i) the discovery FFT which was produced for this object by the selection algorithm, (ii) a phase-fold about 15.685 hours to highlight the eclipse, and (iii) the long-term light curve of this target.

Bibliography

J. Andersen. Accurate masses and radii of normal stars. *The Astronomy and Astrophysics Review*, 3(2):36, 1991.

Alceste Z. Bonanos. Eclispsing binaries: Tools for calibrating the extragalactic distance scale. In *Binary Stars as Critical Tools & Tests*, 2006.

Joshua A. Carter, Saul Rappaport, and Daniel Fabrycky. A third hot white dwarf companion detected by kepler. *The Astrophysical Journal*, 727, 2011.

Jessie Christiansen and Pavel Machalek. *Kepler Data Release 7 Notes.* Data Analysis Working Group, 2010.

Peter P. Eggleton. Approximations to the radii of roche lobes. *The Astrophysical Journal*, 268, May 1983.

Wulff Dieter Heintz. *Double Stars.* D. Reidel Publishing Company, August 1978.

S. Hekker, R. L. Gelliland, Y. Elsworth, and W. J. Chaplin. Characterization of red giant stars in the public *Kepler* data. *Monthly Notices of the Royal Astronomical Society*, 414:2594–2601, 2011.

K. Kolenberg, R. Szabo, D. W. Kurtz, and R. L. Gilliland. First kepler results on rr lyrae stars. *The Astrophysical Journal Letters*, 713(2), 2010.

S.C. Maciel, Y.F.M Osorio, and J.R. DeMedeiros. Ten corot eclipsing binaries: Photometric solutions. *New Astronomy*, 16.

J. M. Nemec, R. Smolec, J. M. Benkő, and P. Moskalik. Fourier analysis of non-blazhko ab-type rr lyrae stars observed with the kepler space telescope. *Monthly Notices of the Royal Astronomical Society*, 417, 2011.

A. J. Norton, S. G. Payne, and T. Evans. Short period eclipsing binary candidates identified using superwasp. *Astronomy and Astrophysics*, January 2011.

Andrej Prša, Natalie Batalha, Robert W. Slawson, and Laurance R. Doyle. Kepler eclipsing binary stars. i. catalog and principal characterization of 1879 eclipsing binaries in the first data release. *The Astronomical Journal*, 141(83):16, March 2011.

S. Rappaport, A. Levine, and E. Chiang. Possible disintegrating short-period super-mercury orbiting kic 12557548. *The Astrophysical Journal*, in press. doi: 10.1088/0004-637X/749/1/1.

J. D. Scargle. Studies in astronomical time series analysis. ii - statistical aspects of spectral analysis of unevenly spaced data. *The Astrophysical Journal*, 263, December 1982.

Robert W. Slawson, Andrej Prša, William F. Welsh, and Jerome A. Orosz. Kepler eclispsing binary stars. ii. 2165 eclipsing binaries in the second data release. *The Astronomical Journal*, 142(160):14, November 2011.